Letter

Coherence-enhanced quantum-dot heat engine

Jaegon Um [1,*] Konstantin E. Dorfman [2,3,4,†] and Hyunggyu Park [5,6,‡]

[1]*Department of Physics, Pohang University of Science and Technology, Pohang 37673, Korea*
[2]*State Key Laboratory of Precision Spectroscopy, East China Normal University, Shanghai 200062, China*
[3]*Collaborative Innovation Center of Extreme Optics, Shanxi University, Taiyuan, Shanxi 030006, People's Republic of China*
[4]*Himalayan Institute for Advanced Study, Unit of Gopinath Seva Foundation, MIG 38, Avas Vikas, Rishikesh, Uttarakhand 249201, India*
[5]*School of Physics, Korea Institute for Advanced Study, Seoul 02455, Korea*
[6]*Quantum Universe Center, Korea Institute for Advanced Study, Seoul 02455, Korea*

(Received 7 December 2021; accepted 2 August 2022; published 25 August 2022)

We show that quantum coherence can enhance the performance of a continuous quantum heat engine in the Lindblad description. We investigate the steady-state solutions of the particle-exchanging quantum heat engine, composed of degenerate double quantum dots coupled to two heat baths in parallel, where quantum coherence may be induced due to interference between relaxation channels. We find that the engine power can be enhanced by the coherence in the nonlinear response regime, when the symmetry of coupling configurations between dots and two baths is broken. In the symmetric case, the coherence cannot be maintained in the steady state, except for the maximum interference degenerate case, where initial-condition-dependent multiple steady states appear with a dark state.

DOI: 10.1103/PhysRevResearch.4.L032034

Introduction. Quantum thermodynamics is an emerging field in view of the significant progress of technology which allows one to scale down heat-energy converting devices to nanoscale where quantum effects become crucial [1]. Examples of such quantum heat engines (QHEs) include lasers, solar cells, and photosynthetic organisms, where, along with a few-level quantum structure [2–4], a phenomenon of quantum coherence plays an important role [5–10]. In particular, coherence in system-bath interactions that originates from the interference may enhance the power [11–13] and efficiency at maximum power [14] of the laser and solar cell and is responsible for highly efficient energy transfer in photosynthetic systems [15]. These effects have been confirmed in the experimental studies of polymer solar cells [16]. The noise-induced coherence is different from the internal coherence in the system Hamiltonian [17], which was recently demonstrated in the nitrogen-vacancy-based microscopic QHE in diamond [18], and manifests as an improved efficiency in spectroscopic pump-probe measurements [19].

So far, the majority of quantum coherence effects has been studied in continuously working bosonic devices [11,12,14,15,20]. Here, we focus on the fermionic QHE autonomously working without an external source, such as driving laser, made up of repulsively interacting double quantum dots with the degenerate energy levels, coupled to fermionic baths in parallel, depicted in Fig. 1. In contrast to previous studies [21–24], we introduce a parameter for the strength of interference between relaxation channels, which plays a crucial role. We derive the condition for maintaining quantum coherence in the steady state and investigate the engine performance, controlled by the tunneling coefficients between dots and baths and the interference strength.

We find that the power enhancement of the QHE can be achieved in the nonlinear response regime [25]. When coupling configurations assigned to each bath are symmetric, a quantum coherence initially induced by interference between relaxation channels would eventually disappear in the long-time (steady-state) limit. The exceptional case emerges for the degenerate energy level configuration at the maximum interference strength, when the dynamics is found to be localized, manifested as a mathematical singularity in the evolution operator evoking the so-called *dark* state [26], characterized by multiple steady states with finite quantum coherence depending on a given initial state. This singularity also emerges in more general settings with coherent dynamics originated from the energy-level degeneracy and parallel couplings, including a single bath case. Note that a spurious quantum coherence can be observed for a very long time (quasistationary state regime) near the maximum interference.

When the coupling configuration symmetry is broken in terms of either tunneling coefficients or interference strengths, a genuine new steady state emerges with nonvanishing quantum coherence, producing a *quantum current* between two baths through dots in addition to the conventional *classical* current. This quantum current yields an extra contribution to the engine power, which can be positive in a specific parameter regime.

Model. We first derive the quantum master equation (QME) [27] for the density operator $\hat{\rho}_S(t)$ of the fermionic QHE in the

*slung@postech.ac.kr
†dorfmank@lps.ecnu.edu.cn
‡hgpark@kias.re.kr

limit of weak coupling to hot (h) and cold (c) baths, where a temperature difference $T_h - T_c > 0$ and a potential bias $\mu_c - \mu_h > 0$ are applied. For simplicity, we assume a single energy level for each quantum dot with the degenerate energy levels $E_1 = E_2 = E$ and infinitely large repulsion between particles in dots. The system then can be described using three two-particle eigenstates: $|0\rangle$ denotes empty dots, and $|1\rangle$ and $|2\rangle$ stand for the occupation of dots 1 and 2, respectively, by a single particle. In addition, coherent hopping between dots is also forbidden and the only source of coherence is due to coupling to thermal baths.

The interaction between system and bath $a(=\mathrm{h}, \mathrm{c})$ is given by $\hat{H}^a_{\mathrm{SB}} = \sum_{d,k} g^a_{dk} \hat{b}^{a\dagger}_k |0\rangle\langle d| + \mathrm{H.c.}$, where $\hat{b}^{a\dagger}_k$ is the operator creating a single particle with momentum k in bath a, and g^a_{dk} is the tunneling coefficient between dot $d(=1,2)$ and bath a. After tracing out bath degrees of freedom with the Born-Markov and the rotating wave approximations (RWA) [27,28], we obtain the QME which reads [29]

$$\partial_t \hat{\rho}_S = -i[\hat{H}_S, \hat{\rho}_S] + \sum_a \sum_{\alpha,\beta=1}^{4} \Gamma^a_{\alpha\beta} \left(\hat{L}_\alpha \hat{\rho}_S \hat{L}^\dagger_\beta - \frac{1}{2}\{\hat{L}^\dagger_\beta \hat{L}_\alpha, \hat{\rho}_S\} \right), \tag{1}$$

where the system Hamiltonian is $\hat{H}_S = E(|1\rangle\langle 1| + |2\rangle\langle 2|)$ and the Lindblad operators are $\hat{L}_1 = |1\rangle\langle 0|$, $\hat{L}_2 = |2\rangle\langle 0|$, $\hat{L}_3 = \hat{L}^\dagger_1$, and $\hat{L}_4 = \hat{L}^\dagger_2$. Note that we neglected the Lamb shift term (see the Supplemental Material [30]). The dissipation matrix Γ^a is given by

$$\Gamma^a = \begin{pmatrix} w^a_{1+} & \phi^a\sqrt{w^a_{1+}w^a_{2+}} & 0 & 0 \\ \phi^{a*}\sqrt{w^a_{1+}w^a_{2+}} & w^a_{2+} & 0 & 0 \\ 0 & 0 & w^a_{1-} & \phi^{a*}\sqrt{w^a_{1-}w^a_{2-}} \\ 0 & 0 & \phi^a\sqrt{w^a_{1-}w^a_{2-}} & w^a_{2-} \end{pmatrix}, \tag{2}$$

where $w^a_{d\pm}$ represents the transfer rate of a particle between dot d and bath a; the subscript $+$ $(-)$ denotes the inflow (outflow) with respect to the dot. These rates are given by $w^a_{d+} = 2\pi|g^a_d|^2 N^a$ and $w^a_{d-} = 2\pi|g^a_d|^2\overline{N^a}$, where $g^a_d = g^a_d(E)$, $N^a = N^a(E)$ is the Fermi-Dirac distribution in bath a and $\overline{N^a} = 1 - N^a$ (see the derivation in Sec. S1 of the Supplemental Material (SM) [30]).

The off-diagonal terms in Eq. (2) represent interference between particle transfer associated with different dots. The interference effect is manifested as the nonzero off-diagonal terms of $\hat{\rho}_S$, e.g., $\langle 1|\hat{\rho}_S|2\rangle \neq 0$. The coherence may not vanish even in the long-time limit due to the degeneracy; otherwise, it could be washed away under the RWA. In realistic experiments, however, the energy levels fluctuate in time due to fluctuations of gate voltages, which is not included in the system Hamiltonian. One expects that energy fluctuations around the degeneracy will result in partial coherence or dephasing [31], which can be phenomenologically added to our QHE model. Considering an observation of the exponentially decaying coherent current in a quantum-dot experiment [32], we introduce a phenomenological parameter ϕ^a representing a dephasing effect due to fluctuating energy levels in Eq. (2), assigned to each bath and which can be estimated experimentally (see Sec. S1 C of the SM [30]); $|\phi^a| = 1$ stands for permitting the full interference of relaxations with bath a, while $\phi^a = 0$ corresponds to no quantum effect of system-bath interactions. In earlier bosonic QHE models, ϕ^a is governed by the angle between dipole moments corresponding to two dots which ensures that $|\phi^a| \leqslant 1$ [11]. For convenience, ϕ^a is treated as a real number. Note that the second term in Eq. (1) is a standard form of the quantum dynamical semigroup [27], which guarantees the positive and trace-preserving dynamics since Γ^a in Eq. (2) is the positive-semidefinite matrix for $|\phi^a| \leqslant 1$.

To solve the QME, it is convenient to map the density operator to a vector: $\mathbf{P} = (\rho_{00}, \rho_{11}, \rho_{22}, \rho_{12}, \rho_{21}, \rho_{01}, \rho_{02}, \rho_{10}, \rho_{20})^{\mathrm{T}}$, where $\rho_{ij} = \langle i|\hat{\rho}_S|j\rangle$. The last four components vanish in the long-time limit because there is no dynamics producing the coherence between the empty and occupied states so that only dephasing is allowed, as seen in Sec. S2 of the SM [30]. Thus, we write the corresponding Liouville equation as

$$\partial_t \mathbf{P} = \mathsf{L}\,\mathbf{P}, \tag{3}$$

where L is a 5×5 matrix with the reduced vector $\mathbf{P} = (\rho_{00}, \rho_{11}, \rho_{22}, \rho_{12}, \rho_{21})^{\mathrm{T}}$. Introducing $W_d = \sum_a w^a_{d+}$, $\overline{W}_d = \sum_a w^a_{d-}$, $\Phi = \sum_a \phi^a\sqrt{w^a_{1+}w^a_{2+}}$, and $\overline{\Phi} = \sum_a \phi^a\sqrt{w^a_{1-}w^a_{2-}}$, the L matrix then reads

$$\mathsf{L} = \begin{pmatrix} -W_1 - W_2 & \overline{W}_1 & \overline{W}_2 & \overline{\Phi} & \overline{\Phi} \\ W_1 & -\overline{W}_1 & 0 & -\overline{\Phi}/2 & -\overline{\Phi}/2 \\ W_2 & 0 & -\overline{W}_2 & -\overline{\Phi}/2 & -\overline{\Phi}/2 \\ \Phi & -\overline{\Phi}/2 & -\overline{\Phi}/2 & -\frac{\overline{W}_1+\overline{W}_2}{2} & 0 \\ \Phi & -\overline{\Phi}/2 & -\overline{\Phi}/2 & 0 & -\frac{\overline{W}_1+\overline{W}_2}{2} \end{pmatrix}. \tag{4}$$

Steady-state solutions. From the steady-state condition, $\mathsf{L}\mathbf{P}(\infty) = 0$, we find the relations as

$$\rho_{11}(\infty) = \frac{W_1\overline{W}_2 - \overline{\Phi}(W_2 + \overline{W}_2 - W_1)\rho_{12}(\infty)}{W_1\overline{W}_2 + \overline{W}_1 W_2 + \overline{W}_1\overline{W}_2},$$
$$\rho_{22}(\infty) = \frac{\overline{W}_1 W_2 - \overline{\Phi}(W_1 + \overline{W}_1 - W_2)\rho_{12}(\infty)}{W_1\overline{W}_2 + \overline{W}_1 W_2 + \overline{W}_1\overline{W}_2}, \tag{5}$$

with the population conservation $(\rho_{00} + \rho_{11} + \rho_{22} = 1)$ and

$$\rho_{12}(\infty) = \rho_{21}(\infty) = \frac{2\Phi - (2\Phi + \overline{\Phi})[\rho_{11}(\infty) + \rho_{22}(\infty)]}{\overline{W}_1 + \overline{W}_2}. \tag{6}$$

Note that the classical solution is recovered from Eq. (5), when the coherence term vanishes $[\rho_{12}(\infty) = 0]$. This clas-

sical *incoherent condition* is determined by Eq. (6) as

$$2\Phi\overline{W}_1\overline{W}_2 - \overline{\Phi}(W_1\overline{W}_2 + \overline{W}_1 W_2) = 0, \tag{7}$$

which is obviously satisfied for the trivial case with $\Phi = \overline{\Phi} = 0$ (or, equivalently, $\phi^a = 0$). Note that the equilibrium case ($T_\mathrm{h} = T_\mathrm{c}$ and $\mu_\mathrm{h} = \mu_\mathrm{c}$) also satisfies this incoherent condition due to $W_d/\overline{W}_d = \Phi/\overline{\Phi}$ with $N^\mathrm{h} = N^\mathrm{c}$.

In general, Eqs. (5) and (6) leads to a 2×2 matrix equation for ρ_{11} and ρ_{22} as

$$\mathsf{L}_\mathrm{ss}\begin{pmatrix}\rho_{11}(\infty)\\ \rho_{22}(\infty)\end{pmatrix} = \begin{pmatrix}W_1 - (2\Phi\overline{\Phi})/(\overline{W}_1 + \overline{W}_2)\\ W_2 - (2\Phi\overline{\Phi})/(\overline{W}_1 + \overline{W}_2)\end{pmatrix}, \tag{8}$$

with

$$\mathsf{L}_\mathrm{ss} = \begin{pmatrix}W_1 + \overline{W}_1 - \frac{\overline{\Phi}(2\Phi+\overline{\Phi})}{\overline{W}_1+\overline{W}_2} & W_1 - \frac{\overline{\Phi}(2\Phi+\overline{\Phi})}{\overline{W}_1+\overline{W}_2}\\ W_2 - \frac{\overline{\Phi}(2\Phi+\overline{\Phi})}{\overline{W}_1+\overline{W}_2} & W_2 + \overline{W}_2 - \frac{\overline{\Phi}(2\Phi+\overline{\Phi})}{\overline{W}_1+\overline{W}_2}\end{pmatrix}. \tag{9}$$

Unless the determinant $|\mathsf{L}_\mathrm{ss}|$ vanishes, the steady-state solution is uniquely defined, which is given explicitly in Eq. (S29) of the SM [30].

We next consider a special *r-symmetric* configuration [22], where the couplings are symmetric for both baths, i.e., $g^\mathrm{h}_2/g^\mathrm{h}_1 = g^\mathrm{c}_2/g^\mathrm{c}_1 \equiv r$, leading to $w^a_{2\pm}/w^a_{1\pm} = r^2$. We take $r > 0$ for simplicity. Assuming an additional symmetry for the coherence parameter as $\phi^\mathrm{h} = \phi^\mathrm{c} \equiv \phi$, one can show $W_d/\overline{W}_d = \Phi/\overline{\Phi}$ even in nonequilibrium ($N^\mathrm{h} \neq N^\mathrm{c}$), satisfying the incoherence condition in Eq. (7). However, at the maximum interference ($|\phi| = 1$), the matrix L_ss becomes singular with $|\mathsf{L}_\mathrm{ss}| = 0$ and multiple steady-state solutions emerge, which will be discussed later. With the broken symmetry ($\phi^\mathrm{h} \neq \phi^\mathrm{c}$), the quantum coherence survives with a nonclassical solution [$\rho_{12}(\infty) \neq 0$]. In a more general case with $g^\mathrm{h}_2/g^\mathrm{h}_1 \neq g^\mathrm{c}_2/g^\mathrm{c}_1$, the classical solution is still possible by adjusting ϕ^h and ϕ^c appropriately to satisfy the incoherent condition, but L_ss cannot be singular.

Steady-state currents. A particle current J^a_d representing the time increment of the particle density of dot d due to bath a can be obtained from Eq. (1) as

$$J^a_d = w^a_{d+}\,\rho_{00} - w^a_{d-}\,\rho_{dd} - \phi^a\sqrt{w^a_{1-}w^a_{2-}}\left(\frac{\rho_{12}+\rho_{21}}{2}\right). \tag{10}$$

In the steady state, J^a_d should be balanced by two reservoirs such that $J^\mathrm{h}_d(\infty) = -J^\mathrm{c}_d(\infty) \equiv J_d(\infty)$ and the total current is given by $J = \sum_d J_d(\infty)$. Transferring an electron from bath h to bath c, the electron gains the energy governed by the difference between the chemical potentials $\mu_\mathrm{c} - \mu_\mathrm{h}$, and thus the QHE power yields $P = (\mu_\mathrm{c} - \mu_\mathrm{h})J$. As the heat flux from bath h is given by $\dot{Q}^\mathrm{h} = (E - \mu_\mathrm{h})J$, the QHE efficiency does not vary with the particle current as $\eta = P/\dot{Q}^\mathrm{h} = (\mu_\mathrm{c} - \mu_\mathrm{h})/(E - \mu_\mathrm{h})$.

The particle current can be further separated into the classical and the quantum parts as

$$J_d(\infty) = J^\mathrm{cl}_d + \Psi_d\,\rho_{12}(\infty), \tag{11}$$

where $\phi^a = 0$ is set for the classical part in Eqs. (5) and (10) as

$$J^\mathrm{cl}_1 = \frac{\Delta N}{|\mathsf{L}_0|}(2\pi)^2|g^\mathrm{h}_1|^2|g^\mathrm{c}_1|^2\overline{W}_2, \quad J^\mathrm{cl}_2 = \frac{\Delta N}{|\mathsf{L}_0|}(2\pi)^2|g^\mathrm{h}_2|^2|g^\mathrm{c}_2|^2\overline{W}_1, \tag{12}$$

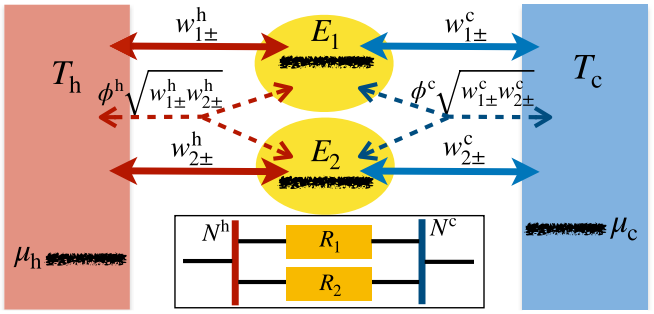

FIG. 1. A schematic illustration of the QHE, composed of two heat baths and a two-dot system. The dot energies, E_1 and E_2 (in this work, $E_1 = E_2$), are higher than the chemical potentials, μ_h and μ_c. $w^a_{d\pm}$ represents the transfer rate of a particle between dot d and bath a, and $\phi^a\sqrt{w^a_{1\pm}w^a_{2\pm}}$ denotes the interference amplitude. Inset: A circuit analogy of resistors in parallel.

with the external (bath) bias $\Delta N \equiv N^\mathrm{h} - N^\mathrm{c}$ and $|\mathsf{L}_0| = W_1\overline{W}_2 + \overline{W}_1 W_2 + \overline{W}_1\overline{W}_2$ [$\mathsf{L}_0 = \mathsf{L}_\mathrm{ss}(\phi^a = 0)$], and $J^\mathrm{cl}_d > 0$ ensuring the positive power requires $\Delta N > 0$.

The second term represents the *quantum current* $J^\mathrm{q}_d \equiv \Psi_d\,\rho_{12}(\infty)$, induced by the coherence, and *quantum speed* Ψ_d and $\rho_{12}(\infty)$ are given in Sec. S3 of the SM [30]. Note that the quantum current for each dot can be both positive and negative, depending on the parameter values, as well as the total quantum current $J^\mathrm{q} = \sum_d J^\mathrm{q}_d$ (see Fig. S1 of the SM [30]).

As $\rho_{12}(\infty)$ is also proportional to bias ΔN, the QHE can be viewed as an analog of an electronic circuit with parallel resistors R_1 and R_2 under the external potential bias (see the inset of Fig. 1). The conductance σ_d of dot d is defined by the Ohm's law of $J_d(\infty) = \sigma_d\Delta N$, which is the reciprocal of resistance as $\sigma_d = R_d^{-1}$. The conductance is also divided into the classical and quantum parts as $\sigma_d = \sigma^\mathrm{cl}_d + \sigma^\mathrm{q}_d$ from Eq. (11). The classical part σ^cl_d is always positive, while the quantum part can be either positive or negative. In Fig. 2, we plot the relative quantum conductance $\sigma^\mathrm{q}_d/\sigma^\mathrm{cl}_d$ in the $(\phi^\mathrm{c}, \phi^\mathrm{h})$

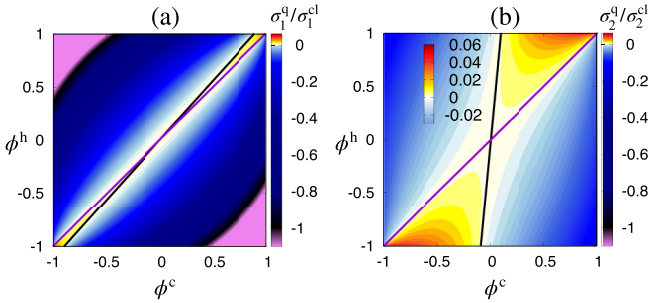

FIG. 2. Relative quantum conductances of (a) dot 1 and (b) dot 2, denoted as $\sigma^\mathrm{q}_1/\sigma^\mathrm{cl}_1$ and $\sigma^\mathrm{q}_2/\sigma^\mathrm{cl}_2$, respectively, in the $(\phi^\mathrm{c}, \phi^\mathrm{h})$ plane. Here, we used $N^\mathrm{h} = 0.2$ and $N^\mathrm{c} = 0.1$, and the r-symmetric configuration with $|g^a_1|^2 = 8\pi/(1+r^2)$ and $|g^a_2|^2 = 8\pi r^2/(1+r^2)$ at $r = 4$. Along the line of symmetry (purple), $\rho_{12}(\infty) = 0$, while $\Psi_d = 0$ defines the black line. The quantum conductances vanish along both lines. Note that a back flow [$J_d(\infty) < 0$] occurs near $\phi^\mathrm{h} = -\phi^\mathrm{c} = \pm 1$ in (a), where the negative quantum current overmatches the positive classical current.

plane in the r-symmetric configuration. Near but off the symmetric line of $\phi^{\rm h} = \phi^{\rm c}$, we find the total quantum conductance $\sigma^{\rm q} = \sum_d \sigma_d^{\rm q} > 0$, which means that the performance of the QHE can be enhanced beyond the classical limit in this parameter regime.

For small ΔN, we expand the relative quantum conductance as

$$\sigma_d^{\rm q}/\sigma_d^{\rm cl} = \mathcal{S}_d^0 + \mathcal{S}_d^1\,\Delta N + \cdots, \tag{13}$$

where $\mathcal{S}_1^0 \sim -(\phi^{\rm h} - \phi^{\rm c})^2$, $\mathcal{S}_2^0 = \mathcal{S}_1^0/r^2$, and $\mathcal{S}_d^1 \sim \phi^{\rm h}(\phi^{\rm h} - \phi^{\rm c})$ for the r-symmetric configuration (see Sec. S3 of the SM [30] for details). Interestingly, $\sigma_d^{\rm q}$ is always nonpositive in the linear response regime ($\mathcal{S}_d^0 \leqslant 0$), but may become positive due to $\mathcal{S}_d^1$ in the nonlinear regime as ΔN increases for $\phi^{\rm h}(\phi^{\rm h} - \phi^{\rm c}) > 0$. Note that $\mathcal{S}_d^1$ can dominate over $\mathcal{S}_d^0$ near the symmetric line ($\phi^{\rm h} = \phi^{\rm c}$). For $r > 1$, the negative quantum effect ($\mathcal{S}_d^0$) is relatively stronger for dot 1, which has a weaker coupling with baths, as also seen in Fig. 2, which might be applicable to a filtering circuit.

Although $\rho_{12}(\infty)$ becomes finite off the symmetric line ($\phi^{\rm h} \neq \phi^{\rm c}$), the quantum current may vanish again when $\Psi_d = 0$ in Eq. (11), which is denoted by black lines in Fig. 2. This can happen by balancing the quantum contributions from the stochastic part and the interference part, which are represented by the first two terms and the third term in the right-hand side of Eq. (10), respectively. The quantum enhancement occurs only between two lines of $\Psi_d = 0$ and $\rho_{12}(\infty) = 0$. For general cases outside of the r-symmetric configuration, these two lines are simply tilted (see Fig. S1 in the SM [30]), but the general features of the QHE are essentially unchanged.

Coupling-configuration symmetric case. We focus on the symmetric case with $\phi^{\rm h} = \phi^{\rm c} = \phi$ in the r-symmetric configuration, where $W_2 = r^2 W_1$, $\overline{W}_2 = r^2 \overline{W}_1$, $\Phi = r\phi W_1$, and $\overline{\Phi} = r\phi\overline{W}_1$, yielding $W_d/\overline{W}_d = \Phi/\overline{\Phi}$. Then, the QME in Eq. (1) can be reduced to the single *effective* bath case, defined by a single coherence parameter ϕ and a rate W_1. A single bath typically enforces the system to reach a classical equilibrium state in the long-time limit. However, with degenerate energy levels, the off-diagonal (coherent) terms in the dissipation matrix Γ in Eq. (2) cannot be ignored even under the RWA. Thus, these coherent terms slow down the quantum dynamics significantly ($|\phi| < 1$), approaching the classical steady state via a long-lived quasistationary state with nonzero coherence.

We first calculate the eigenvectors $\mathbf{v}_i$ and the corresponding eigenvalues λ_i of the Liouville matrix L. Details are given in Sec. S4 of the SM [30]. We find the steady-state eigenvector $\mathbf{v}_1^{\rm T} = (\bar{\alpha}, \alpha, \alpha, 0, 0)$ with $\lambda_1 = 0$, where $\alpha = W_1/(2W_1 + \overline{W}_1)$ and $\bar{\alpha} = 1 - 2\alpha$, which corresponds to the classical fixed point. Other eigenvalues are negative except for $|\phi| = 1$, and thus the classical fixed point represents the unique steady state. At $|\phi| = 1$, however, another eigenvector $\mathbf{v}_4$ also has the zero eigenvalue, allowing multiple fixed points spanned by $\mathbf{v}_1$ and $\mathbf{v}_4$. Note that $|\mathsf{L}_{\rm ss}| = r^2(1-\phi^2)(2W_1 + \overline{W}_1)\overline{W}_1$ from Eq. (9), which vanishes at these singular points of $|\phi| = 1$.

Defining a matrix $\mathsf{V} = (\mathbf{v}_1, \mathbf{v}_2, \mathbf{v}_3, \mathbf{v}_4, \mathbf{v}_5)$, the formal solution for $\mathbf{P}(t)$ reads

$$\mathbf{P}(t) = \mathsf{V}(1,\ \chi_2 e^{\lambda_2 t},\ \chi_3 e^{\lambda_3 t},\ \chi_4 e^{\lambda_4 t},\ \chi_5 e^{\lambda_5 t})^{\rm T}, \tag{14}$$

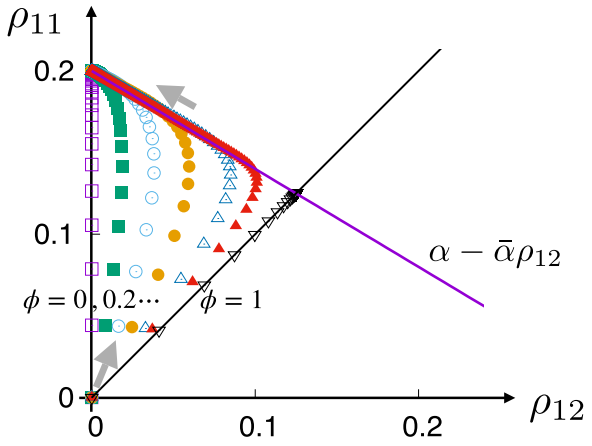

FIG. 3. Dynamic trajectories starting from $(\rho_{12}, \rho_{11}) = (0, 0)$ for various ϕ with $r = 1$, $W_1 = 0.25$, and $\overline{W}_1 = 0.75$, yielding $\alpha = 0.2$ and $\bar{\alpha} = 0.6$. Numerical data are denoted by various symbols for $\phi = 0, 0.2, 0.4, 0.6, 0.8, 0.9, 1$ (from left to right). The time interval between the same symbols is set to be 0.2 and the gray arrows denote the direction of the dynamics. The classical fixed point is at $(\rho_{12}, \rho_{11}) = (0, 0.2)$, while the coherent fixed point is at (0.125,0.125).

where χ_i depends on the initial condition $\mathbf{P}(0)$. At $|\phi| = 1$, $\lambda_1 = \lambda_4 = 0$, the steady state $\mathbf{P}(\infty)$ depends on $\mathbf{P}(0)$. In Fig. 3, we display typical dynamic trajectories in the (ρ_{12}, ρ_{11}) space with $r = 1$, starting from the empty initial condition of $\rho_{ij}(0) = 0$ except for $\rho_{00}(0) = 1$. As expected, all trajectories end up in the single (classical) fixed point in the long-time limit except for $|\phi| = 1$, where the new coherent fixed point appears with $\rho_{12}(\infty) \neq 0$. Note that the dynamics for $\phi \lesssim 1$ detours around the coherent fixed point for a significantly long time (quasistationary state), approaching the classical fixed point, which allows for experimental observation even in the presence of small decoherence.

The additional zero eigenvalue ($\lambda_4 = 0$) at the singular points ($|\phi| = 1$) implies another conservation law in addition to the probability conservation. Specifically, we find $r^2\dot{\rho}_{11} + \dot{\rho}_{22} - r\dot{\rho}_{12} - r\dot{\rho}_{21} = 0$ for $\phi = 1$ from Eq. (4), or $r^2\rho_{11}(t) + \rho_{22}(t) - r\rho_{12}(t) - r\rho_{21}(t) = I_0$ for all time t, where I_0 is a constant determined by the initial condition. We obtain the steady-state solutions using Eq. (5) and the conservation law, written as $\rho_{11}(\infty) = \alpha - [r\bar{\alpha} - \frac{1-r^2}{r}\alpha]\,\rho_{12}(\infty)$ and $\rho_{22}(\infty) = \alpha - [\frac{\bar{\alpha}}{r} + \frac{1-r^2}{r}\alpha]\,\rho_{12}(\infty)$, with

$$\rho_{12}(\infty) = \rho_{21}(\infty) = \frac{r}{1+r^2}\frac{1}{1-\alpha}\left(\alpha - \frac{I_0}{1+r^2}\right), \tag{15}$$

which depends on the initial state. In Fig. 3, we set $r = 1$ and $I_0 = 0$, so the coherent fixed point is determined by the intersection of two lines, $\rho_{11} = \rho_{12}$ and $\rho_{11} = \alpha - \bar{\alpha}\rho_{12}$. For $I_0 \neq 0$, the coherent fixed point is shifted along the curve of $\rho_{11} = \alpha - \bar{\alpha}\rho_{12}$. The case of $\phi = -1$ yields the same results except for changing the signs of ρ_{12} and ρ_{21} (see Eq. (S61) of the SM [30]). Note that the coherence can be finite and initial-state dependent even for $\Delta N = 0$ (equilibrium). This may raise a doubt that the quantum current $J_d^{\rm q}$

might not vanish in equilibrium, which is not the case since the quantum speed Ψ_d is proportional to bias ΔN (in fact, $\Psi_d = \phi(\frac{1+r^2}{r})J_d^{\rm cl}$ in Eq. (S62) of the SM [30]). The relative quantum conductance can be positive even in the linear response regime, i.e., $\mathcal{S}_d^0$ can be positive, depending on the initial state.

The phenomena of multiple fixed points responsible for a *dark* state emergence are observed in both fermionic [22] and bosonic [26,33] systems. Here, the system state can be recast in a rotated orthonormal basis as $|0\rangle$, $|+\rangle = (|1\rangle + r|2\rangle)/\mathcal{N}_r$, and $|-\rangle = (r|1\rangle - |2\rangle)/\mathcal{N}_r$ with $\mathcal{N}_r = \sqrt{1+r^2}$. Then, the system Hamiltonian is given as $\hat{H}_{\rm S} = E(|+\rangle\langle+| + |-\rangle\langle-|)$ and the interaction Hamiltonian becomes $\hat{H}^a_{\rm SB} = \mathcal{N}_r \sum_k g^a_{1k}\hat{b}^{a\dagger}_k|0\rangle\langle+| + {\rm H.c.}$ at the singular points. Note that the state $|-\rangle$ remains unchanged under the evolution operator, which corresponds to the dark state at $\phi = 1$, i.e., any initial population in the dark state remains intact or $\langle-|\hat{\rho}_{\rm S}|-\rangle = (r^2\rho_{11} + \rho_{22} - r\rho_{12} - r\rho_{21})/\mathcal{N}_r^2$ should be conserved. We can easily extend our result to the degenerate multiple dots with multiple occupancy allowed. As the dark state decouples with baths, it may be useful to protect quantum information from decoherence [34].

Note that the Lindblad description of degenerate quantum dots coupled to a single bath also yields multiple steady states with coherence at the maximum interference, in contrast with the common knowledge that a system coupled to a single bath should reach the incoherent thermal equilibrium, regardless of its initial state. Thus, the phenomenological parameter ϕ is natural to guarantee the thermal steady state for $|\phi| < 1$. Near the singular points, one may observe a long-living quasistationary state with the information of initial-state-dependent coherent solutions.

Conclusion. We investigated all possible steady-state solutions for the continuous quantum-dot QHE coupled to terminals in parallel for various tunneling coefficients and interference strengths. Here, the interference strength plays a similar role of the alignment of dipoles [35] in the bosonic system and acts as a source of decoherence. We found that unless the interference is completely negated, the steady states possess the coherence, which generates an extra quantum current, resulting in the enhanced QHE performance in a specific region of the parameter space, where the nonpositive linear quantum conductance is overcome by nonlinear contributions. We remark that a fine tuning of the parameter values is necessary for a significant enhancement such as the near symmetric coupling parameters. More enhanced QHE may require further investigation for the origin of nonlinear quantum conductance. Recently, the single-quantum-dot (fermion) heat engine was realized experimentally [36]. Since double-quantum-dot systems coupled to baths in parallel have been studied experimentally [37–39], the parallel-double-dot engine is also expected to be synthesized to confirm the enhancement of the QHE performance by thermal noises.

Acknowledgments. This research was supported by the NRF Grants No. 2020R1I1A1A01071924 (J.U.), No. 2017R1D1A1B06035497 (H.P.), and No. 2022R1I1A1A01063166 (J.U.), and by the KIAS individual Grant No. PG013604 (H.P.). K.E.D. is supported by the National Science Foundation of China (Grant No. 11934011), the Zijiang Endowed Young Scholar Fund, the East China Normal University, and the Overseas Expertise Introduction Project for Discipline Innovation (111 Project, Grant No. B12024).

[1] G. Benenti, G. Casati, K. Saito, and R. S. Whitney, Fundamental aspects of steady-state conversion of heat to work at the nanoscale, Phys. Rep. **694**, 1 (2017).

[2] M. O. Scully, M. S. Zubairy, G. S. Agarwal, and H. Walther, Extracting work from a single heat bath via vanishing quantum coherence, Science **299**, 862 (2003).

[3] R. Kosloff and A. Levy, Quantum heat engines and refrigerators: Continuous devices, Annu. Rev. Phys. Chem. **65**, 365 (2014).

[4] J. Jaramillo, M. Beau, and A. del Campo, Quantum supremacy of many-particle thermal machines, New J. Phys. **18**, 075019 (2016).

[5] H.-B. Chen, P.-Y. Chiu, and Y.-N. Chen, Vibration-induced coherence enhancement of the performance of a biological quantum heat engine, Phys. Rev. E **94**, 052101 (2016).

[6] R. S. Whitney, Quantum coherent three-terminal thermoelectrics: Maximum efficiency at given power output, Entropy **18**, 208 (2016).

[7] B. K. Agarwalla, J.-H. Jiang, and D. Segal, Quantum efficiency bound for continuous heat engines coupled to noncanonical reservoirs, Phys. Rev. B **96**, 104304 (2017).

[8] N. Brunner, M. Huber, N. Linden, S. Popescu, R. Silva, and P. Skrzypczyk, Entanglement enhances cooling in microscopic quantum refrigerators, Phys. Rev. E **89**, 032115 (2014).

[9] M. T. Mitchison, M. P. Woods, J. Prior, and M. Huber, Coherence-assisted single-shot cooling by quantum absorption refrigerators, New J. Phys. **17**, 115013 (2015).

[10] K. Hammam, Y. Hassouni, R. Fazio, and G. Manzano, Optimizing autonomous thermal machines powered by energetic coherence, New J. Phys. **23**, 043024 (2021).

[11] M. O. Scully, K. R. Chapin, K. E. Dorfman, M. B. Kim, and A. Svidzinsky, Quantum heat engine power can be increased by noise-induced coherence, Proc. Natl. Acad. Sci. USA **108**, 15097 (2011).

[12] Y. Yao, Spin-boson theory for charge photogeneration in organic molecules: Role of quantum coherence, Phys. Rev. B **91**, 045421 (2015).

[13] C. L. Latune, I. Sinayskiy, and F. Petruccione, Thermodynamics from indistinguishability: Mitigating and amplifying the effects of the bath, Phys. Rev. Research **1**, 033192 (2019).

[14] K. E. Dorfman, D. Xu, and J. Cao, Efficiency at maximum power of a laser quantum heat engine enhanced by noise-induced coherence, Phys. Rev. E **97**, 042120 (2018).

[15] K. E. Dorfman, D. V. Voronine, S. Mukamel, and M. O. Scully, Photosynthetic reaction center as a quantum heat engine, Proc. Natl. Acad. Sci. USA **110**, 2746 (2013).

[16] E. R. Bittner and C. Silva, Noise-induced quantum coherence drives photo-carrier generation dynamics at polymeric

semiconductor heterojunctions, Nat. Commun. **5**, 3119 (2014).

[17] R. Uzdin, A. Levy, and R. Kosloff, Equivalence of Quantum Heat Machines, and Quantum-Thermodynamic Signatures, Phys. Rev. X **5**, 031044 (2015).

[18] J. Klatzow, J. N. Becker, P. M. Ledingham, C. Weinzetl, K. T. Kaczmarek, D. J. Saunders, J. Nunn, I. A. Walmsley, R. Uzdin, and E. Poem, Experimental Demonstration of Quantum Effects in the Operation of Microscopic Heat Engines, Phys. Rev. Lett. **122**, 110601 (2019).

[19] Md. Qutubuddin and K. E. Dorfman, Incoherent control of optical signals: Quantum-heat-engine approach, Phys. Rev. Research **3**, 023029 (2021); Incoherent control of two-photon induced optical measurements in open quantum systems Quantum heat engine perspective, **4**, 023259 (2022).

[20] V. Holubec and T. Novotný, Effects of noise-induced coherence on the performance of quantum absorption refrigerators, J. Low Temp. Phys. **192**, 147 (2018).

[21] U. Harbola, M. Esposito, and S. Mukamel, Quantum master equation for electron transport through quantum dots and single molecules, Phys. Rev. B **74**, 235309 (2006).

[22] G. Schaller, G. Kießlich, and T. Brandes, Transport statistics of interacting double dot systems: Coherent and non-Markovian effects, Phys. Rev. B **80**, 245107 (2009).

[23] G. B. Cuetara, M. Esposito, and G. Schaller, Quantum thermodynamics with degenerate eigenstate coherences, Entropy **18**, 447 (2016).

[24] F. D. Ribetto, R. A. Bustos-Marún, and H. L. Calvo, Role of coherence in quantum-dot-based nanomachines within the Coulomb blockade regime, Phys. Rev. B **103**, 155435 (2021).

[25] A similar result was reported in a cyclic bosonic QHE; see K. Brandner, M. Bauer, and U. Seifert, Universal Coherence-Induced Power Losses of Quantum Heat Engines in Linear Response, Phys. Rev. Lett. **119**, 170602 (2017).

[26] V. V. Kozlov, Y. Rostovtsev, and M. O. Scully, Inducing quantum coherence via decays and incoherent pumping with application to population trapping, lasing without inversion, and quenching of spontaneous emission, Phys. Rev. A **74**, 063829 (2006).

[27] H.-P. Breuer and F. Petruccione, *The Theory of Open Quantum Systems* (Oxford University Press, New York, 2002).

[28] R. Alicki and R. Kosloff, Introduction to quantum thermodynamics: History and prospects, in *Thermodynamics in the Quantum Regime*, edited by F. Binder *et al.* (Springer, Cham, 2018), pp. 1–33.

[29] For the additivity of baths in the QME, see, also, X.-Q. Li, J. Y. Luo, Y.-G. Yang, P. Cui, and Y. J. Yan, Quantum master-equation approach to quantum transport through mesoscopic systems, Phys. Rev. B **71**, 205304 (2005); K. Ptaszyński, Coherence-enhanced constancy of a quantum thermoelectric generator, **98**, 085425 (2018); M. T. Mitchison and M. B. Plenio, Non-additive dissipation in open quantum networks out of equilibrium, New J. Phys. **20**, 033005 (2018).

[30] See Supplemental Material at http://link.aps.org/supplemental/10.1103/PhysRevResearch.4.L032034 for the derivation of the QME, eigenfunction analysis of the Liouville operator, calculations of steady-state currents, and analysis of the fully symmetric case.

[31] M. Q. Weng, Decoherence and relaxation in the interacting quantum dot system, Europhys. Lett. **85**, 17003 (2009).

[32] T. Hayashi, T. Fujisawa, H. D. Cheong, Y. H. Jeong, and Y. Hirayama, Coherent Manipulation of Electronic States in a Double Quantum Dot, Phys. Rev. Lett. **91**, 226804 (2003).

[33] J. Thingna, D. Manzano, and J. Cao, Dynamical signatures of molecular symmetries in nonequilibrium quantum transport, Sci. Rep. **6**, 28027 (2016).

[34] M. Zanner, T. Orell, C. M. F. Schneider, R. Albert, S. Oleschko, M. L. Juan, M. Silveri, and G. Kirchmair, Coherent control of a multi-qubit dark state in waveguide quantum electrodynamics, Nat. Phys. **18**, 538 (2022).

[35] A. A. Svidzinsky, K. E. Dorfman, and M. O. Scully, Enhancing photocell power by noise-induced coherence, Coher. Phenom. **1**, 7 (2012).

[36] M. Josefsson, A. Svilans, A. M. Burke, E. A. Hoffmann, S. Fahlvik, C. Thelander, M. Leijnse and H. Linke, A quantum-dot heat engine operating close to the thermodynamic efficiency limits, Nat. Nanotechnol. **13**, 920 (2018).

[37] A. W. Holleitner, C. R. Decker, H. Qin, K. Eberl, and R. H. Blick, Coherent Coupling of Two Quantum Dots Embedded in an Aharonov-Bohm Interferometer, Phys. Rev. Lett. **87**, 256802 (2001).

[38] A. W. Holleitner, R. H. Blick, A. K. Hüttel, K. Eberl, and J. P. Kotthaus, Probing and controlling the bonds of an artificial molecule, Science **297**, 70 (2002).

[39] J. C. Chen, A. M. Chang, and M. R. Melloch, Transition between Quantum States in a Parallel-Coupled Double Quantum Dot, Phys. Rev. Lett. **92**, 176801 (2004).

Supplementary Material for

"Coherence enhanced quantum-dot heat engine"

Jaegon Um*

Department of Physics, Pohang University of Science and Technology, Pohang 37673, Korea

Konstantin E. Dorfman†

State Key Laboratory of Precision Spectroscopy,

East China Normal University, Shanghai 200062, China

Hyunggyu Park‡

School of Physics, Korea Institute for Advanced Study, Seoul 02455, Korea and

Quantum Universe Center, Korea Institute for Advanced Study, Seoul 02455, Korea

* slung@postech.ac.kr

† dorfmank@lps.ecnu.edu.cn

‡ hgpark@kias.re.kr

S1. QUANTUM MASTER EQUATION

A. Model

We start with the Hamiltonian for the system (quantum dots) interacting with heat baths, which are given by

$$\hat{H} = \hat{H}_{\rm S} + \hat{H}_{\rm B} + \hat{H}_{\rm SB}\,, \tag{S1}$$

where $\hat{H}_{\rm S}$, $\hat{H}_{\rm B}$, and $\hat{H}_{\rm SB}$ denote the Hamiltonians for the quantum-dot system, heat baths and interactions between the system and baths, respectively. The Hamiltonian of double quantum dots is given by

$$\hat{H}_{\rm S} = E_1\hat{d}_1^\dagger\hat{d}_1 + E_2\hat{d}_2^\dagger\hat{d}_2 + E_{12}\hat{d}_1^\dagger\hat{d}_1\hat{d}_2^\dagger\hat{d}_2\,, \tag{S2}$$

where E_1 and E_2 denote energies for dot 1 and dot 2, respectively, and E_{12} is the Coulomb repulsion between electrons at dots. In the case of the degenerated dots, $E_1 = E_2 \equiv E$. Here $\hat{d}_d$ ($\hat{d}_d^\dagger$) is the fermionic operator annihilating (creating) a single particle at dot d. We assume that only a single spinless fermion is allowed for each dot. Note that coherent hoppings between dots are not allowed.

The bath Hamiltonian is the sum of each bath Hamiltonian $\hat{H}_{\rm B}^a$ of bath a , which can be also written in terms of fermionic operators as

$$\hat{H}_{\rm B} = \sum_{a={\rm h,c}} \hat{H}_{\rm B}^a = \sum_{a={\rm h,c}}\sum_k \omega_k^a\,\hat{b}_k^{a\dagger}\hat{b}_k^a\,, \tag{S3}$$

where $\hat{b}_k^a$ ($\hat{b}_k^{a\dagger}$) denotes the operator annihilating (creating) a particle with momentum k and energy ω_k^a in bath a (for simplicity, we assume here that the momentum is a scalar variable). The interaction Hamiltonian $H_{\rm SB}$ is also the simple sum of the interaction Hamiltonian $\hat{H}_{\rm SB}^a$ for each bath a, which is also expressed with the fermionic operators as

$$\hat{H}_{\rm SB} = \sum_{a={\rm h,c}} \hat{H}_{\rm SB}^a = \sum_{a={\rm h,c}}\sum_{d=1,2}\sum_k g_{dk}^a\,\hat{b}_k^{a\dagger}\hat{d}_d \;+ h.c.\,, \tag{S4}$$

which describes an electron hopping between dot d and bath a with a coupling strength $g_{dk}^a \equiv g_d^a(\omega_k^a)$, depending on the momentum or energy.

In the limit of $E_{12} \to \infty$ (infinite repulsion), the simultaneous occupation at both dots is prohibited, thus the system state can be described with the three orthonormal bases of $|0\rangle$ (empty), $|1\rangle$ (single occupation in dot 1), and $|2\rangle$ (single occupation in dot 2). Then, the operator $\hat{d}_d$ at dot d

can be replaced by a jump operator $|0\rangle\langle d|$. Using these bases, we rewrite

$$\hat{H}_{\rm S} = E_0|0\rangle\langle 0| + E_1|1\rangle\langle 1| + E_2|2\rangle\langle 2|\,, \quad \hat{H}_{\rm SB} = \sum_a \sum_{d,k} g^a_{dk}\, \hat{b}^{a\dagger}_k |0\rangle\langle d| + h.c. \tag{S5}$$

where E_0 means the empty-state energy (here, we set $E_0 = 0$).

B. Derivation of the QME

We derive the QME with an assumption that dots and baths are weakly coupled [1]. Instead of exploiting fermionic operators of dots, used in previous works [2–4], we use the jump operators. Starting from the von Neumann equation of the total system, $\partial_t\hat{\rho} = -{\rm i}\left[\hat{H}, \hat{\rho}\right]$, where $\hat{\rho}(t)$ is the density operator in the Schrödinger picture, the system dynamics expressed by the reduced density operator, $\hat{\rho}_{\rm S} = {\rm tr}_{\rm B}\,\hat{\rho}$, is obtained by tracing out the bath degrees of freedom in the total system dynamic equation. In the weak coupling limit where the interaction Hamiltonian is small in comparison to the system and bath Hamiltonian, it is convenient to take the interaction picture, where $\hat{\rho}'(t) = e^{{\rm i}(\hat{H}_{\rm S}+\hat{H}_{\rm B})t}\hat{\rho}(t)e^{-{\rm i}(\hat{H}_{\rm S}+\hat{H}_{\rm B})t}$ with $\hat{\rho}(t) = e^{-{\rm i}\hat{H}t}\hat{\rho}(0)e^{i\hat{H}t}$. Then, the von Neumann equation in the interaction picture becomes

$$\partial_t\hat{\rho}' = -{\rm i}\left[\hat{H}'_{\rm SB}, \hat{\rho}'\right], \tag{S6}$$

where the interaction Hamiltonian in the interaction picture $\hat{H}'_{\rm SB} = e^{{\rm i}(\hat{H}_{\rm S}+\hat{H}_{\rm B})t}\hat{H}_{\rm SB}e^{-{\rm i}(\hat{H}_{\rm S}+\hat{H}_{\rm B})t}$ is obtained from Eq. (S5) as

$$\hat{H}'_{\rm SB} = \sum_a \sum_{d,k}\left[g^a_{dk}\, e^{{\rm i}\hat{H}_{\rm B}t}\,\hat{b}^{a\dagger}_k e^{-{\rm i}\hat{H}_{\rm B}t}\,|0\rangle\langle d|\, e^{-{\rm i}E_d t} + h.c.\right]. \tag{S7}$$

Using a formal solution, $\hat{\rho}'(t) = \hat{\rho}(0) - {\rm i}\int_0^t d\tau[\hat{H}'_{\rm SB}(\tau), \hat{\rho}'(\tau)]$, the equation for $\hat{\rho}'_{\rm S} = {\rm tr}_{\rm B}\,\hat{\rho}'$ is written as

$$\partial_t\hat{\rho}'_{\rm S}(t) = -{\rm tr}_{\rm B}\int_0^t d\tau\,\left[\hat{H}'_{\rm SB}(t), \left[\hat{H}'_{\rm SB}(\tau), \hat{\rho}'(\tau)\right]\right], \tag{S8}$$

where the initial condition satisfies ${\rm tr}_{\rm B}[\hat{H}'_{\rm SB}, \hat{\rho}'(0)] = 0$. Substituting $\tau = t - s$, we obtain

$$\partial_t\hat{\rho}'_{\rm S}(t) = -{\rm tr}_{\rm B}\int_0^t ds\,\left[\hat{H}'_{\rm SB}(t), \left[\hat{H}'_{\rm SB}(t-s), \hat{\rho}'(t-s)\right]\right]. \tag{S9}$$

Now we take the so-called Born-Markov approximation, where it is assumed that $\hat{\rho}'(t) \approx \hat{\rho}'_{\rm S}(t)\otimes\hat{\rho}_{\rm B}$ with the canonical heat bath density operator,

$$\hat{\rho}_{\rm B} = Z^{-1}e^{-\sum_a\left(\hat{H}^a_{\rm B} - \mu_a\hat{n}_a\right)/T_a}, \tag{S10}$$

with the temperature T_a, the chemical potential μ_a, and the number operator $\hat{n}_a = \sum_k \hat{b}_k^{a\dagger}\hat{b}_k^a$ for each bath a, and the partition function $Z = \mathrm{tr}_\mathrm{B} e^{-\sum_a (\hat{H}_\mathrm{B}^a - \mu_a \hat{n}_a)/T_a}$ (the Boltzmann constant is set as $k_\mathrm{B} = 1$). As the total density operator is given in the product form, this assumption implies that each bath is always in its equilibrium, regardless of the system evolution. This happens when the bath time scale τ_B^a is much smaller than the system time scale, thus the time scale separation between the system and baths is taken for granted, leading to the approximate replacement of $\hat{\rho}'_\mathrm{S}(t-s) \to \hat{\rho}'_\mathrm{S}(t)$. Since the correlation $\mathrm{tr}_\mathrm{B}\left[\hat{H}'_\mathrm{SB}(t), \left[\hat{H}'_\mathrm{SB}(t-s), \hat{\rho}'(t)\right]\right]$ in Eq. (S9) may vanish for $s \gg \tau_\mathrm{B}^a$, the integral upper bound can be extended to ∞, yielding a simpler approximate dynamic equation as

$$\partial_t \hat{\rho}'_\mathrm{S}(t) = -\mathrm{tr}_\mathrm{B} \int_0^\infty ds \left[\hat{H}'_\mathrm{SB}(t), \left[\hat{H}'_\mathrm{SB}(t-s), \hat{\rho}'_\mathrm{S}(t) \otimes \hat{\rho}_B\right]\right]. \tag{S11}$$

Inserting Eq. (S7) into Eq.(S11), one can write each term in the commutation in Eq. (S11) as

$$\begin{aligned}
\mathrm{tr}_\mathrm{B} \hat{H}'_\mathrm{SB}(t)\hat{H}'_\mathrm{SB}(t-s)\hat{\rho}'_\mathrm{S}(t) \otimes \hat{\rho}_\mathrm{B} = \sum_{a,k}\Bigg[\sum_d \Big[|g_{dk}^a|^2 \left(C_k^a(s)\, e^{-\mathrm{i}E_d s} |0\rangle\langle 0| + D_k^a(s)\, e^{\mathrm{i}E_d s} |d\rangle\langle d| \right)\Big] \\
+ g_{1k}^{a*} g_{2k}^a\, D_k^a(s)\, e^{\mathrm{i}(E_1-E_2)t} e^{\mathrm{i}E_2 s} |1\rangle\langle 2| + g_{1k}^a g_{2k}^{a*}\, D_k^a(s)\, e^{-\mathrm{i}(E_1-E_2)t} e^{\mathrm{i}E_1 s} |2\rangle\langle 1| \Big]\, \hat{\rho}'_\mathrm{S}\,,
\end{aligned} \tag{S12}$$

$$\begin{aligned}
\mathrm{tr}_\mathrm{B} \hat{H}'_\mathrm{SB}(t)\hat{\rho}'_\mathrm{S}(t) \otimes \hat{\rho}_\mathrm{B}\hat{H}'_\mathrm{SB}(t-s) = \sum_{a,k}\Bigg[\sum_d \Big[|g_{dk}^a|^2 \left(D_k^a(-s) e^{-\mathrm{i}E_d s} |0\rangle\langle d| \hat{\rho'}_\mathrm{S} |d\rangle\langle 0| + C_k^a(-s) e^{\mathrm{i}E_d s} |d\rangle\langle 0| \hat{\rho}'_\mathrm{S} |0\rangle\langle d| \right)\Big] \\
+ g_{1k}^{a*} g_{2k}^a \left(D_k^a(-s) e^{\mathrm{i}(E_1-E_2)t} e^{-\mathrm{i}E_1 s} |0\rangle\langle 2| \hat{\rho}'_\mathrm{S} |1\rangle\langle 0| + C_k^a(-s) e^{\mathrm{i}(E_1-E_2)t} e^{\mathrm{i}E_2 s} |1\rangle\langle 0| \hat{\rho}'_\mathrm{S} |0\rangle\langle 2| \right) \\
+ g_{1k}^a g_{2k}^{a*} \left(D_k^a(-s) e^{-\mathrm{i}(E_1-E_2)t} e^{-\mathrm{i}E_2 s} |0\rangle\langle 1| \hat{\rho}'_\mathrm{S} |2\rangle\langle 0| + C_k^a(-s) e^{\mathrm{i}(E_1-E_2)t} e^{\mathrm{i}E_2 s} |2\rangle\langle 0| \hat{\rho}'_\mathrm{S} |0\rangle\langle 1| \right)\Big]\,,
\end{aligned} \tag{S13}$$

and the remainders are the Hermitian conjugates of Eqs. (S12) and (S13). Note that each bath contributes additively to Eq. (S11). and the correlators for bath a are defined by

$$C_k^a(s) = \mathrm{tr}_\mathrm{B}\, e^{\mathrm{i}\hat{H}_\mathrm{B} s} \hat{b}_k^{a\dagger} e^{-\mathrm{i}\hat{H}_\mathrm{B} s}\, \hat{b}_k^a \hat{\rho}_\mathrm{B} \quad \text{and} \quad D_k^a(s) = \mathrm{tr}_\mathrm{B}\, e^{\mathrm{i}\hat{H}_\mathrm{B} s}\, \hat{b}_k^a\, e^{-\mathrm{i}\hat{H}_\mathrm{B} s} \hat{b}_k^{a\dagger} \hat{\rho}_\mathrm{B}\,. \tag{S14}$$

With the Fock-state description of bath particles in Eq. (S10), we find

$$C_k^a(s) = N^a(\omega_k^a) e^{\mathrm{i}\omega_k^a s} \quad \text{and} \quad D_k^a(s) = \left[1 - N^a(\omega_k^a)\right] e^{-\mathrm{i}\omega_k^a s} \tag{S15}$$

where N_a is the Fermi-Dirac distribution in bath a, given as

$$N^a(\omega) = \frac{\exp[-(\omega-\mu_a)/T_a]}{1+\exp[-(\omega-\mu_a)/T_a]}. \tag{S16}$$

Since the integral over time s in Eq. (S11) yields the delta function, i.e.,

$$\int_0^\infty ds e^{\pm \mathrm{i}(\omega_k^a - E_d)s} = \pi\delta(\omega_k^a - E_d)\,, \tag{S17}$$

a single mode for each bath satisfying $\omega_k^a = E$ survives in Eq. (S11) for the degenerate case with $E_1 = E_2 = E$. Note that we have omitted the Lamb shift correction, which is the order of E^{-1}, negligible in the high energy limit.

Changing $\sum_k \to \mathcal{N}\int dk$ with a proper normalization $\mathcal{N}$ and integrating over k, we calculate the transition rates. First, consider the incoherent terms such as $|d\rangle\langle 0|\hat{\rho}'_{\rm S}|0\rangle\langle d|$ and $|0\rangle\langle d|\hat{\rho}'_{\rm S}|d\rangle\langle 0|$. For transitions between $|0\rangle$ and $|d\rangle$ due to bath a, the transitions rates are obtained as

$$w_{d+}^a = 2\pi|g_d^a|^2 N^a(E) \quad \text{and} \quad w_{d-}^a = 2\pi|g_d^a|^2\overline{N^a}(E)\,, \tag{S18}$$

where $\overline{N^a} = 1 - N^a$ and $g_d^a = g_d^a(E)$. Note that $g_d^a(E) = g_{dk}^a$ with $\omega_k^a = E$. The + sign in Eq. (S18) stands for the transition from $|0\rangle$ to $|d\rangle$ and the $-$ sign stands for the opposite direction. Now we consider interference terms such as $|0\rangle\langle 2|\hat{\rho}'_{\rm S}|1\rangle\langle 0|$ or $|1\rangle\langle 0|\hat{\rho}'_{\rm S}|0\rangle\langle 2|$. Due to the phase factor $\exp[\pm{\rm i}(E_1 - E_2)t]$, the interference terms vanish in long-time limit unless $E_1 = E_2$ (rotating wave approximation). In this work with $E_1 = E_2 = E$, we find the nonvanishing interference terms as

$$\sqrt{w_{1+}^a w_{2+}^a}\,e^{\pm{\rm i}\theta^a} \quad \text{and} \quad \sqrt{w_{1-}^a w_{2-}^a}\,e^{\pm{\rm i}\theta^a}\,, \tag{S19}$$

where θ^a is the difference of phase angles between g_1^a and g_2^a, defined as $g_1^{a*}g_2^a = |g_1^a||g_2^a|e^{{\rm i}\theta^a}$.

Defining the Lindblad operators as

$$\hat{L}_1 = |1\rangle\langle 0|\,, \quad \hat{L}_2 = |2\rangle\langle 0|\,, \quad \hat{L}_3 = |0\rangle\langle 1|\,, \quad \hat{L}_4 = |0\rangle\langle 2|\,, \tag{S20}$$

the dynamic equation for the density operator in Eq. (S11) is rewritten as

$$\begin{aligned}
\partial_t\hat{\rho}'_{\rm S} = \sum_a \Bigg[& w_{1+}^a\left(\hat{L}_1\hat{\rho}'_{\rm S}\hat{L}_1^\dagger - \frac{1}{2}\left\{\hat{L}_1^\dagger\hat{L}_1, \hat{\rho}'_{\rm S}\right\}\right) + w_{2+}^a\left(\hat{L}_2\hat{\rho}'_{\rm S}\hat{L}_2^\dagger - \frac{1}{2}\left\{\hat{L}_2^\dagger\hat{L}_2, \hat{\rho}'_{\rm S}\right\}\right) \\
& + w_{1-}^a\left(\hat{L}_3\hat{\rho}'_{\rm S}\hat{L}_3^\dagger - \frac{1}{2}\left\{\hat{L}_3^\dagger\hat{L}_3, \hat{\rho}'_{\rm S}\right\}\right) + w_{2-}^a\left(\hat{L}_4\hat{\rho}'_{\rm S}\hat{L}_4^\dagger - \frac{1}{2}\left\{\hat{L}_4^\dagger\hat{L}_4, \hat{\rho}'_{\rm S}\right\}\right) \\
& + \sqrt{w_{1+}^a w_{2+}^a}\,e^{{\rm i}\theta^a}\hat{L}_1\hat{\rho}'_{\rm S}\hat{L}_2^\dagger + \sqrt{w_{1+}^a w_{2+}^a}\,e^{-{\rm i}\theta^a}\hat{L}_2\hat{\rho}'_{\rm S}\hat{L}_1^\dagger \\
& + \sqrt{w_{1-}^a w_{2-}^a}\,e^{-{\rm i}\theta^a}\left(\hat{L}_3\hat{\rho}'_{\rm S}\hat{L}_4^\dagger - \frac{1}{2}\left\{\hat{L}_4^\dagger\hat{L}_3, \hat{\rho}'_{\rm S}0\right\}\right) + \sqrt{w_{1-}^a w_{2-}^a}\,e^{{\rm i}\theta^a}\left(\hat{L}_4\hat{\rho}'_{\rm S}\hat{L}_3^\dagger - \frac{1}{2}\left\{\hat{L}_3^\dagger\hat{L}_4, \hat{\rho}'_{\rm S}\right\}\right)\Bigg]\,,
\end{aligned} \tag{S21}$$

where $\{\,,\}$ denotes the anticommutator. We introduce a phenomenological prefactor ϕ_a for the interference terms in Eq. (S21) by replacing $e^{{\rm i}\theta^a} \to \phi^a$ with $|\phi^a| \le 1$ to take into account decoherence effects by other unknown environmental noises [5]. Note that the phase difference θ^a is absorbed into ϕ^a. In the Schrödinger picture with $\hat{\rho}_{\rm S}(t) = e^{-{\rm i}\hat{H}_{\rm S}t}\hat{\rho}'_{\rm S}(t)e^{{\rm i}\hat{H}_{\rm S}t}$, Eq. (S21) is rewritten as a matrix form in Eqs. (1) and (2) of the main text.

C. Origin and experimental relevance of ϕ^a

Before solving Eq. (1), we discuss the origin of ϕ^a and its experimental relevance. In the derivation of Eq. (S21), we assumed the degenerate levels, $E_1 = E_2 = E$, which allows electrons in dots to retain coherence induced by Eq. (S19) even in the long-time limit. In realistic situations, however, there may exist fluctuations in energy levels, influenced by uncontrollable external noises, which may damage the induced coherence (dephasing).

Experimental quantification of the dephasing effect induced by fluctuating energies was reported by measuring the tunnelling current through coherently coupled quantum dots under a pulse train [6], where the coherent current is reduced by a factor of $\exp\left(-\tau_{\rm p}/\tau_{\rm D}\right)$ with the pulse duration time $\tau_{\rm p}$ and the dephasing time $\tau_{\rm D}$ (see Eq. (2) in [6]). In the experiment, coherent and incoherent processes are separated in time and the coherent process is allowed while the pulse is applied during $\tau_{\rm p}$. Thus, given the dephasing rate, the decaying of the coherent current depends on the duration time of coherent process. By varying τ_p, the dephasing time $\tau_{\rm D}$ can be estimated by fitting experimental data for the tunnelling current in the above exponential form.

In our model, where quantum dots interact with baths coherently, a single-electron tunnelling between a bath and dots itself is a coherent process. Every term in r.h.s of Eq. (S21) can be regarded as micro currents due to the single tunnellings and thus, interference terms with $\sqrt{w^a_{1\pm}w^a_{2\pm}}$ represent coherent currents, which may suffer from dephasing in the presence of energy fluctuations. We assume that the energy fluctuation is not so strong as to modify transition rates $w^a_{d\pm}$, whereas it evokes an exponentially decaying factor for interference terms in functions of the dephasing time and the coherent tunnelling time. To estimate the tunnelling time, suppose a round trip of a single electron; starting from bath a, it hops into dots and comes back to bath a. For simplicity, we ignore the other bath, then the typical time scale for the trip can be obtained by the sum of the inverse transition rates, i.e. $1/w^a_{d+} + 1/w^a_{d-}$. The average tunnelling (coherent) time τ^a is then estimated as

$$\tau^a \sim \frac{1}{2}\max\left\{\left(2\pi|g^a_1|^2 N^a\overline{N^a}\right)^{-1}, \left(2\pi|g^a_2|^2 N^a\overline{N^a}\right)^{-1}\right\}, \tag{S22}$$

which plays a role of the coherent time τ_p in the above example. Then, the interference terms should be dressed with a dephasing factor ϕ^a as

$$e^{{\rm i}\theta^a}\sqrt{w^a_{1\pm}w^a_{2\pm}} \to \phi^a\sqrt{w^a_{1\pm}w^a_{2\pm}} \quad \text{with} \quad |\phi^a| \sim \exp\left(-\tau^a/\tau_{\rm D}\right). \tag{S23}$$

From Eqs. (S22) and (S23), one can see that ϕ^a can be controlled through the coupling coefficient g^a_d which can be tuned by adjusting a gate voltage between dot d and bath a [7]. Similar to the

above example, it is possible to test the exponential decay form of Eq. (S23) by varying τ^a (actually g_d^a) in experiments for double quantum dots coupled to baths in parallel [8–10]. It is reasonable to assume that the dephasing time $\tau_{\rm D}$ does not depend on τ^a in the same experimental set-up and thus one can estimate $\tau_{\rm D}$ by fitting experimental data into the exponential form. With this information on $\tau_{\rm D}$, one can investigate the ϕ^a-dependence of the coherent current in experiments by simply tuning gate voltages.

S2. EIGENVECTORS AND EIGENVALUES OF THE LIOUVILLE OPERATOR

The density operator can be written in a form of vector: $\mathbf{P} = (\rho_{00}, \rho_{11}, \rho_{22}, \rho_{12}, \rho_{21}, \rho_{01}, \rho_{02}, \rho_{10}, \rho_{20})^{\rm T}$, with $\rho_{ij} = \langle i|\hat{\rho}_{\rm S}|j\rangle$. Then, the equation of motion is given by $\partial_t \mathbf{P} = \mathsf{L}^{\rm tot}\,\mathbf{P}$, where the Liouville operator $\mathsf{L}^{\rm tot}$ has a form of

$$\mathsf{L}^{\rm tot} = \begin{pmatrix} \mathsf{L} & 0 \\ 0 & \mathsf{L}_{\rm irr} + \mathsf{E} \end{pmatrix}, \tag{S24}$$

where the upper 5×5 block is given by $\mathsf{L} = \sum_a \mathsf{L}^a$ and the first term of the lower 4×4 block $\mathsf{L}_{\rm irr} = \sum_a \mathsf{L}^a_{\rm irr}$. Each term in the summation is given as

$$\mathsf{L}^a = \begin{pmatrix} -\left(w^a_{1+}+w^a_{2+}\right) & w^a_{1-} & w^a_{2-} & \phi^{a*}\sqrt{w^a_{1-}w^a_{2-}} & \phi^a\sqrt{w^a_{1-}w^a_{2-}} \\ w^a_{1+} & -w^a_{1-} & 0 & -\phi^{a*}\sqrt{w^a_{1-}w^a_{2-}}/2 & -\phi^a\sqrt{w^a_{1-}w^a_{2-}}/2 \\ w^a_{2+} & 0 & -w^a_{2-} & -\phi^{a*}\sqrt{w^a_{1-}w^a_{2-}}/2 & -\phi^a\sqrt{w^a_{1-}w^a_{2-}}/2 \\ \phi^a\sqrt{w^a_{1+}w^a_{2+}} & -\phi^a\sqrt{w^a_{1-}w^a_{2-}}/2 & -\phi^a\sqrt{w^a_{1-}w^a_{2-}}/2 & -\left(w^a_{1-}+w^a_{2-}\right)/2 & 0 \\ \phi^{a*}\sqrt{w^a_{1+}w^a_{2+}} & -\phi^{a*}\sqrt{w^a_{1-}w^a_{2-}}/2 & -\phi^{a*}\sqrt{w^a_{1-}w^a_{2-}}/2 & 0 & -\left(w^a_{1-}+w^a_{2-}\right)/2 \end{pmatrix}, \tag{S25}$$

$$\mathsf{L}^a_{\rm irr} = \begin{pmatrix} -\left(w^a_{1+}+w^a_{2+}+w^a_{1-}\right)/2 & -\phi^{a*}\sqrt{w^a_{1-}w^a_{2-}}/2 & 0 & 0 \\ -\phi^a\sqrt{w^a_{1-}w^a_{2-}}/2 & -\left(w^a_{1+}+w^a_{2+}+w^a_{2-}\right)/2 & 0 & 0 \\ 0 & 0 & -\left(w^a_{1+}+w^a_{2+}+w^a_{1-}\right)/2 & -\phi^a\sqrt{w^a_{1-}w^a_{2-}}/2 \\ 0 & 0 & -\phi^{a*}\sqrt{w^a_{1-}w^a_{2-}}/2 & -\left(w^a_{1+}+w^a_{2+}+w^a_{2-}\right)/2 \end{pmatrix}, \tag{S26}$$

and the second term of the lower block E is

$$\mathsf{E} = \begin{pmatrix} iE & 0 & 0 & 0 \\ 0 & iE & 0 & 0 \\ 0 & 0 & -iE & 0 \\ 0 & 0 & 0 & -iE \end{pmatrix}. \tag{S27}$$

It is easy to see that each 2×2 subblock of $\mathsf{L}^a_{\rm irr}$ has negative eigenvalues only for $|\phi^a| \leq 1$, thus ρ_{01}, ρ_{02}, ρ_{10}, and ρ_{20}, associated with $\mathsf{L}_{\rm irr}$ will vanish in long-time limit as the pure imaginary E contributes to a modulation only.

From now on, we focus on the 5×5 matrix L with the reduced vector $\mathbf{P} = (\rho_{00}, \rho_{11}, \rho_{22}, \rho_{12}, \rho_{21})^{\rm T}$, satisfying the dynamic equation $\partial_t \mathbf{P} = \mathsf{L}\,\mathbf{P}$. For convenience, we take ϕ^a as a real number. We introduce collective parameters for the sake of brevity as

$$W_d = \sum_a w^a_{d+}\,, \quad \overline{W}_d = \sum_a w^a_{d-}\,, \quad \Phi = \sum_a \phi^a \sqrt{w^a_{1+} w^a_{2+}}\,, \quad \overline{\Phi} = \sum_a \phi^a \sqrt{w^a_{1-} w^a_{2-}}\,, \tag{S28}$$

and then Eq. (4) of the main text is obtained.

From Eq. (8), we find the steady-state solution by inverting the 2×2 matrix $\mathsf{L}_{\rm ss}$ when its determinant $|\mathsf{L}_{\rm ss}| \neq 0$ as

$$\begin{aligned}
\rho_{11}(\infty) &= \frac{W_1\overline{W}_2 - \overline{\Phi}\left[2\Phi\overline{W}_2 + \overline{\Phi}\,(W_1 - W_2)\right]/\left(\overline{W}_1 + \overline{W}_2\right)}{|\mathsf{L}_{\rm ss}|}\,, \\
\rho_{22}(\infty) &= \frac{\overline{W}_1 W_2 - \overline{\Phi}\left[2\Phi\overline{W}_1 + \overline{\Phi}\,(W_2 - W_1)\right]/\left(\overline{W}_1 + \overline{W}_2\right)}{|\mathsf{L}_{\rm ss}|}\,, \\
\rho_{12}(\infty) = \rho_{21}(\infty) &= \frac{2\Phi\overline{W}_1\overline{W}_2 - \overline{\Phi}\left(W_1\overline{W}_2 + \overline{W}_1 W_2\right)}{|\mathsf{L}_{\rm ss}|\left(\overline{W}_1 + \overline{W}_2\right)}\,,
\end{aligned} \tag{S29}$$

with

$$|\mathsf{L}_{\rm ss}| = W_1\overline{W}_2 + \overline{W}_1 W_2 + \overline{W}_1\overline{W}_2 - \overline{\Phi}\left(2\Phi + \overline{\Phi}\right)\,, \tag{S30}$$

and ρ_{00} can be obtained from the probability conservation of $\rho_{00} = 1 - \rho_{11} - \rho_{22}$. This steady-state solution should correspond to the eigenvector $\mathbf{v}_1$ of the L matrix with the eigenvalue $\lambda_1 = 0$, where

$$\mathbf{v}_1 = (\rho_{00}(\infty), \rho_{11}(\infty), \rho_{22}(\infty), \rho_{12}(\infty), \rho_{12}(\infty))^{\rm T}\,. \tag{S31}$$

The other eigenvectors and eigenvalues are reported as below for completeness. The two eigenvectors, $\mathbf{v}_2$ and $\mathbf{v}_3$, have the degenerate eigenvalues $\lambda_2 = \lambda_3 = -\left(\overline{W}_1 + \overline{W}_2\right)/2$, where

$$\mathbf{v}_2 = (0, 0, 0, 1, -1)^{\rm T} \quad \text{and} \quad \mathbf{v}_3 = \left(0, 1, -1, \frac{\overline{W}_2 - \overline{W}_1}{2\bar{\Phi}}, \frac{\overline{W}_2 - \overline{W}_1}{2\bar{\Phi}}\right)^{\rm T}\,. \tag{S32}$$

The eigenvalues of the remaining two eigenvectors are the two roots of the characteristic equation of $\lambda^2 + \lambda\left(W_1 + \overline{W}_1 + W_2 + \overline{W}_2\right) + |\mathsf{L}_{\rm ss}| = 0$. Thus, we find the eigenvalues λ_4 and λ_5 as

$$\lambda_{4,5} = \frac{-\left(W_1 + \overline{W}_1 + W_2 + \overline{W}_2\right) \pm U}{2}\,, \tag{S33}$$

with $U = \sqrt{\left(W_1 + \overline{W}_1 + W_2 + \overline{W}_2\right)^2 - 4|\mathsf{L}_{\rm ss}|}$, where λ_4 and λ_5 correspond to the + and − sign, respectively. The explicit expressions for $\mathbf{v}_4$ and $\mathbf{v}_5$ are shown as

$$\mathbf{v}_{4(5)} = \left(1, -\frac{\lambda_{4(5)} + W_2 + \overline{W}_2 - W_1}{2\lambda_{4(5)} + \overline{W}_1 + \overline{W}_2}, -\frac{\lambda_{4(5)} + W_1 + \overline{W}_1 - W_2}{2\lambda_{4(5)} + \overline{W}_1 + \overline{W}_2}, \frac{2\Phi + \overline{\Phi}}{2\lambda_{4(5)} + \overline{W}_1 + \overline{W}_2}, \frac{2\Phi + \overline{\Phi}}{2\lambda_{4(5)} + \overline{W}_1 + \overline{W}_2}\right)^{\mathrm{T}}. \tag{S34}$$

Note that $|\mathsf{L}_{\rm ss}| = 0$ yields the additional zero eigenvalue, $\lambda_4 = 0$ and we expect multiple steady-state solutions given by a linear combination of $\mathbf{v}_1$ and $\mathbf{v}_4$.

S3. STEADY-STATE CURRENTS

In this section, we calculate steady-state currents explicitly. The net particle currents J_d^a from bath a to dot d can be calculated from the Liouville equation in Eqs. (3) and (4) of the main text by sorting out the contributions to the time increment of the particle density of each dot d ($\dot{\rho}_{dd}$) from each bath a. Then, we can easily identify

$$J_d^a(t) = w_{d+}^a \rho_{00}(t) - w_{d-}^a \rho_{dd}(t) - \phi^a \sqrt{w_{1-}^a w_{2-}^a} \left(\frac{\rho_{12}(t) + \rho_{21}(t)}{2}\right) \tag{S35}$$

where the first term in the right-hand-side represents particle transfer from bath a to the empty dot d, the second term represents particle transfer form the occupied dot d to bath a, and finally the third term represents the interference between relaxation channels to both dots. In the steady state, the particle density at dots is stationary, so the currents from both baths should be balanced in such a way that $J_d^{\rm h}(\infty) = -J_d^{\rm c}(\infty) \equiv J_d(\infty)$.

We can divide the particle current into the classical and quantum part as

$$J_d(\infty) = J_d^{\rm cl} + J_d^{\rm q} = J_d^{\rm cl} + \Psi_d \rho_{12}(\infty), \tag{S36}$$

where the quantum current $J_d^{\rm q}$ is given as a product of the *quantum speed* Ψ_d and the coherence $\rho_{12}(\infty)$. The classical current is easily obtained by simply setting $\phi^a = 0$ in Eq. (S35) and Eq. (5) of the main text, and using the rates $w_{d+}^a = 2\pi|g_d^a|^2 N^a$ and $w_{d-}^a = 2\pi|g_d^a|^2\overline{N^a}$, yielding

$$J_1^{\rm cl} = \frac{1}{|\mathsf{L}_0|}\left(w_{1+}^{\rm h}\overline{W}_1 - w_{1-}^{\rm h} W_1\right)\overline{W}_2 = \frac{\Delta N}{|\mathsf{L}_0|}(2\pi)^2 |g_1^{\rm h}|^2 |g_1^{\rm c}|^2 \overline{W}_2\,, \tag{S37}$$

$$J_2^{\rm cl} = \frac{1}{|\mathsf{L}_0|}\left(w_{2+}^{\rm h}\overline{W}_2 - w_{2-}^{\rm h} W_2\right)\overline{W}_1 = \frac{\Delta N}{|\mathsf{L}_0|}(2\pi)^2 |g_2^{\rm h}|^2 |g_2^{\rm c}|^2 \overline{W}_1\,, \tag{S38}$$

where $|\mathsf{L}_0| = |\mathsf{L}_{\rm ss}|_{\phi^a=0} = W_1\overline{W}_2 + \overline{W}_1 W_2 + \overline{W}_1\overline{W}_2$ and the external bias $\Delta N = N^{\rm h} - N^{\rm c} > 0$. Note that $J_d^{\rm cl}$ is always positive. The quantum part, $J_d^{\rm q} = \Psi_d \rho_{12}(\infty)$, is also obtained from Eq. (S35) and

Eq. (5) of the main text, yielding

$$\Psi_1 = \frac{\overline{\Phi}}{|\mathsf{L}_0|}\left[\left(w^{\rm h}_{1+}\overline{W}_1 - w^{\rm h}_{1-}W_1\right) + w^{\rm h}_{1-}W_2 + \left(w^{\rm h}_{1+} + w^{\rm h}_{1-}\right)\overline{W}_2\right] - \phi^{\rm h}\sqrt{w^a_{1-}w^a_{2-}}\,, \tag{S39}$$

$$\Psi_2 = \frac{\overline{\Phi}}{|\mathsf{L}_0|}\left[\left(w^{\rm h}_{2+}\overline{W}_2 - w^{\rm h}_{2-}W_2\right) + w^{\rm h}_{2-}W_1 + \left(w^{\rm h}_{2+} + w^{\rm h}_{2-}\right)\overline{W}_1\right] - \phi^{\rm h}\sqrt{w^a_{1-}w^a_{2-}}\,, \tag{S40}$$

and the coherence term $\rho_{12}(\infty) = \rho_{21}(\infty)$ is obtained from Eq. (S29), after some algebra, as

$$\rho_{12}(\infty) = \frac{\Delta N(2\pi)^2}{|\mathsf{L}_{\rm ss}|}\frac{|g^{\rm h}_1||g^{\rm h}_2|\phi^{\rm h}\left(|g^{\rm c}_2|^2\overline{W}_1 + |g^{\rm c}_1|^2\overline{W}_2\right) - |g^{\rm c}_1||g^{\rm c}_2|\phi^{\rm c}\left(|g^{\rm h}_2|^2\overline{W}_1 + |g^{\rm h}_1|^2\overline{W}_2\right)}{\overline{W}_1 + \overline{W}_2}\,, \tag{S41}$$

which is valid except for the singular case of $|\mathsf{L}_{\rm ss}| = 0$ (see Sec. S4 for the singular case). In contrast to the classical current, the quantum current $J^{\rm q}_d$ can be both positive and negative, which can vanish either by the zero quantum speed ($\Psi_d = 0$) or by the zero coherence ($\rho_{12} = 0$). In Fig. 2 of the main text, the lines of $\Psi_d = 0$ and $\rho_{12}(\infty) = 0$ are plotted in the $(\phi^{\rm c}, \phi^{\rm h})$ plane for the r-symmetric configuration. Note that the $\Psi_d = 0$ lines can be different from each other. For the total quantum current $J^{\rm q} = \sum_d J^{\rm q}_d = \Psi\rho_{12}(\infty)$ with $\Psi = \sum_d \Psi_d$, the lines of $\Psi = 0$ and $\rho_{12}(\infty) = 0$ are shown in Fig. S1, where $J^{\rm q} > 0$ is accomplished only in the shaded area with the same signs of Ψ and $\rho_{12}(\infty)$. Therefore, the engine performance can be enhanced due to the extra positive quantum current in a specific region of the parameter space.

As can be seen in Eqs. (S37), (S38), and (S41), both the classical and quantum current are proportional to the external bias ΔN. Thus, it is natural to define the conductance σ_d for dot d as $J_d(\infty) \equiv \sigma_d\,\Delta N$, which is also divided into the classical and quantum contribution as $\sigma_d = \sigma^{\rm cl}_d + \sigma^{\rm q}_d$. The classical conductance $\sigma^{\rm cl}_d$ can be easily obtained from Eqs. (S37) and (S38), which is always positive ($\sigma^{\rm cl}_d > 0$). The quantum conductance can be obtained from Eqs. (S39), (S40), and (S41). It would be interesting to study the total quantum conductance $\sigma^{\rm q} = \sum_d \sigma^{\rm q}_d$ in the linear response regime for small bias ΔN. For convenience, we introduce the mean bias $N \equiv (N^{\rm h} + N^{\rm c})/2$ with $\overline{N} \equiv 1 - N$. After some algebra, we find

$$\lim_{\Delta N\to 0}\sigma^{\rm q} = -\frac{(2\pi)^2\left[|g^{\rm h}_1||g^{\rm h}_2|\phi^{\rm h}\left(|g^{\rm c}_2|^2\overline{W}^{\rm eq}_1 + |g^{\rm c}_1|^2\overline{W}^{\rm eq}_2\right) - |g^{\rm c}_1||g^{\rm c}_2|\phi^{\rm c}\left(|g^{\rm h}_2|^2\overline{W}^{\rm eq}_1 + |g^{\rm h}_1|^2\overline{W}^{\rm eq}_2\right)\right]^2}{\left(|g^{\rm h}_1|^2 + |g^{\rm c}_1|^2\right)\left(|g^{\rm h}_2|^2 + |g^{\rm c}_2|^2\right)\left(\overline{W}^{\rm eq}_1 + \overline{W}^{\rm eq}_2\right)|\mathsf{L}_{\rm ss}|^{\rm eq}}\,, \tag{S42}$$

where $\overline{W}^{\rm eq}_d = 2\pi\overline{N}\left(|g^{\rm h}_d|^2 + |g^{\rm c}_d|^2\right)$ and $|\mathsf{L}_{\rm ss}|^{\rm eq}$ from Eq. (S30) as

$$|\mathsf{L}_{\rm ss}|^{\rm eq} = (2\pi)^2(1+N)\overline{N}\left[\left(|g^{\rm h}_1|^2 + |g^{\rm c}_1|^2\right)\left(|g^{\rm h}_2|^2 + |g^{\rm c}_2|^2\right) - \left(|g^{\rm h}_1||g^{\rm h}_2|\,\phi^{\rm h} + |g^{\rm c}_1||g^{\rm c}_2|\,\phi^{\rm c}\right)^2\right].$$

Note that the quantum conductance in Eq. (S42) cannot be positive, implying the current enhancement is not possible in the linear response regime.

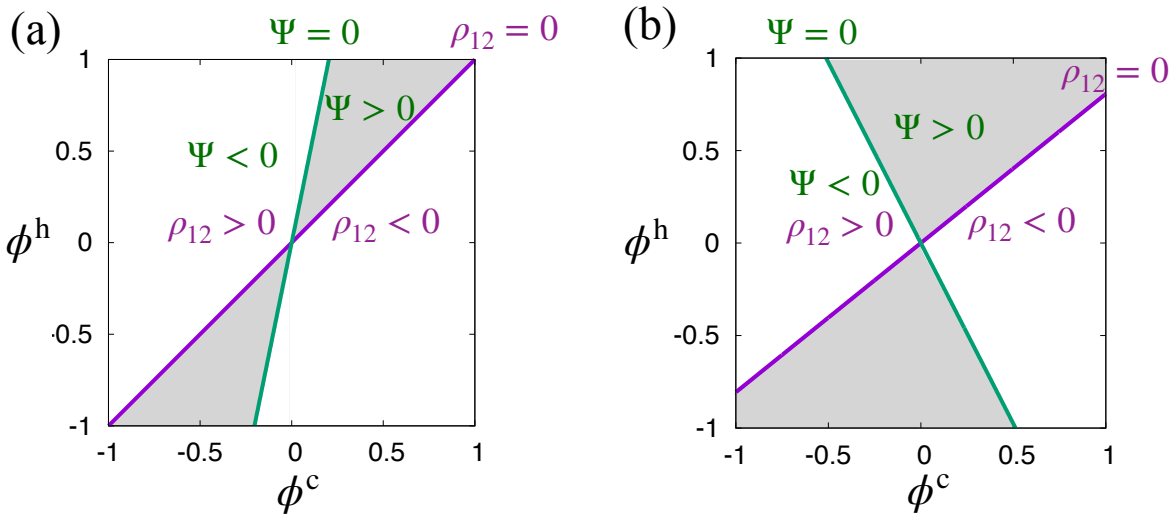

FIG. S1. Lines of vanishing quantum currents ($J^{\rm q} = \Psi\rho_{12}(\infty) = 0$) in the $(\phi^{\rm c}, \phi^{\rm h})$ plane. The purple line represents $\rho_{12}(\infty) = 0$ and the green line represents $\Psi = 0$. The engine performance is enhanced by the extra quantum current in the shaded regions ($J_{\rm q} > 0$). We used $N^{\rm h} = 0.25$, $N^{\rm c} = 0.1$ and tunneling coefficients as $g_1^{\rm h} = g_1^{\rm c} = 1/\sqrt{2\pi}$ for dot 1 and (a) $g_2^{\rm h} = g_2^{\rm c} = 4/\sqrt{2\pi}$ (r-symmetric configuration with $r = 4$) and (b) $g_2^{\rm h} = 12/\sqrt{2\pi}$ and $g_2^{\rm c} = 4/\sqrt{2\pi}$ (r-symmetry broken) for dot 2.

Next, we will investigate the nonlinear regime in the r-symmetric configuration ($g_2^a = rg_1^a$), where the algebra becomes simplified. From Eqs. (S37) and (S38), we can easily see that the classical currents for two dots are simply related as $J_2^{\rm cl} = r^2 J_1^{\rm cl}$. For convenience, we set the tunnelling coefficients as

$$|g_1^a|^2 = \frac{k^a}{1+r^2}\,, \quad |g_2^a|^2 = \frac{r^2 k^a}{1+r^2}\,, \tag{S43}$$

which satisfies the r-symmetric condition. Then, we find

$$\sigma_1^{\rm cl} = \frac{2\pi}{1+r^2}\frac{k^{\rm h}k^{\rm c}}{k^{\rm h}\widetilde{N}^{\rm h} + k^{\rm c}\widetilde{N}^{\rm c}}\,, \quad \sigma_2^{\rm cl} = r^2\sigma_1^{\rm cl}\,, \tag{S44}$$

where $\widetilde{N}^a = 1 + N^a$. After some algebra, we also find the relative quantum conductance $\sigma_d^{\rm q}/\sigma_d^{\rm cl}$ as

$$\begin{aligned}\frac{\sigma_1^{\rm q}}{\sigma_1^{\rm cl}} = \frac{r^2}{1+r^2}\frac{2\left(\phi^{\rm h}-\phi^{\rm c}\right)}{\mathcal{L}}\frac{k^{\rm h}k^{\rm c}}{k^{\rm h}\overline{N}^{\rm h} + k^{\rm c}\overline{N}^{\rm c}}\Big[\phi^{\rm c}\left\{\left(k^{\rm h}+k^{\rm c}\right) - \left(k^{\rm h}N^{\rm h} + k^{\rm c}N^{\rm c}\right)N^{\rm h}\right\}\overline{N}^{\rm c} \\ -\phi^{\rm h}\left\{\left(k^{\rm h}+k^{\rm c}\right) - \left(k^{\rm h}N^{\rm h} + k^{\rm c}N^{\rm c}\right)N^{\rm c}\right\}\overline{N}^{\rm h}\Big] \\ + \frac{1}{1+r^2}\frac{2\left(\phi^{\rm h}-\phi^{\rm c}\right)}{\mathcal{L}}\frac{k^{\rm h}k^{\rm c}}{k^{\rm h}\overline{N}^{\rm h} + k^{\rm c}\overline{N}^{\rm c}}\left(\phi^{\rm h}k^{\rm h}\overline{N}^{\rm h} + \phi^{\rm c}k^{\rm c}\overline{N}^{\rm c}\right)\left(N^{\rm h}-N^{\rm c}\right)\,,\end{aligned} \tag{S45}$$

$$\frac{\sigma_2^{\rm q}}{\sigma_2^{\rm cl}} = \frac{1}{1+r^2}\frac{2\left(\phi^{\rm h}-\phi^{\rm c}\right)}{\mathcal{L}}\frac{k^{\rm h}k^{\rm c}}{k^{\rm h}\overline{N}^{\rm h}+k^{\rm c}\overline{N}^{\rm c}}\Big[\phi^{\rm c}\left\{\left(k^{\rm h}+k^{\rm c}\right)-\left(k^{\rm h}N^{\rm h}+k^{\rm c}N^{\rm c}\right)N^{\rm h}\right\}\overline{N}^{\rm c} \\ -\phi^{\rm h}\left\{\left(k^{\rm h}+k^{\rm c}\right)-\left(k^{\rm h}N^{\rm h}+k^{\rm c}N^{\rm c}\right)N^{\rm c}\right\}\overline{N}^{\rm h}\Big] \\ +\frac{r^2}{1+r^2}\frac{2\left(\phi^{\rm h}-\phi^{\rm c}\right)}{\mathcal{L}}\frac{k^{\rm h}k^{\rm c}}{k^{\rm h}\overline{N}^{\rm h}+k^{\rm c}\overline{N}^{\rm c}}\left(\phi^{\rm h}k^{\rm h}\overline{N}^{\rm h}+\phi^{\rm c}k^{\rm c}\overline{N}^{\rm c}\right)\left(N^{\rm h}-N^{\rm c}\right), \tag{S46}$$

where $\mathcal{L}$ reads

$$\mathcal{L} = \left(k^{\rm h}\overline{N}^{\rm h}+k^{\rm c}\overline{N}^{\rm c}\right)\left(k^{\rm h}\widetilde{N}^{\rm h}+k^{\rm c}\widetilde{N}^{\rm c}\right)-\left(k^{\rm h}\phi^{\rm h}\overline{N}^{\rm h}+k^{\rm c}\phi^{\rm c}\overline{N}^{\rm c}\right)\left(k^{\rm h}\phi^{\rm h}\widetilde{N}^{\rm h}+k^{\rm c}\phi^{\rm c}\widetilde{N}^{\rm c}\right). \tag{S47}$$

In the expansion of $\sigma_d^{\rm q}/\sigma_d^{\rm cl} = \mathcal{S}_d^0 + \mathcal{S}_d^1\,\Delta N + O(\Delta N^2)$, the leading terms are given by

$$\mathcal{S}_1^0 = -\frac{r^2}{1+r^2}\frac{2k^{\rm h}k^{\rm c}(1-N^2)}{\mathcal{L}^{\rm eq}}\left(\phi^{\rm h}-\phi^{\rm c}\right)^2, \quad \mathcal{S}_2^0 = -\frac{1}{1+r^2}\frac{2k^{\rm h}k^{\rm c}(1-N^2)}{\mathcal{L}^{\rm eq}}\left(\phi^{\rm h}-\phi^{\rm c}\right)^2, \tag{S48}$$

where $\mathcal{L}^{\rm eq} = \left(1-N^2\right)\left[\left(k^{\rm h}+k^{\rm c}\right)^2-\left(k^{\rm h}\phi^{\rm h}+k^{\rm c}\phi^{\rm c}\right)^2\right]$.

Setting $\phi^{\rm c} = \phi - \Delta\phi$ and $\phi^{\rm h} = \phi$ with a finite ϕ, we obtain

$$\mathcal{S}_1^1 = \frac{r^2}{1+r^2}\frac{2k^{\rm h}k^{\rm c}\phi\Delta\phi + O(\Delta\phi^2)}{\mathcal{L}^{\rm eq}} + \frac{1}{1+r^2}\frac{2k^{\rm h}k^{\rm c}\phi\Delta\phi + O'(\Delta\phi^2)}{\mathcal{L}^{\rm eq}} \\ \approx \frac{2k^{\rm h}k^{\rm c}\phi\Delta\phi}{(1-N^2)\left(k^{\rm h}+k^{\rm c}\right)^2\left(1-\phi^2\right)}, \tag{S49}$$

and

$$\mathcal{S}_2^1 = \frac{1}{1+r^2}\frac{2k^{\rm h}k^{\rm c}\phi\Delta\phi + O(\Delta\phi^2)}{\mathcal{L}^{\rm eq}} + \frac{r^2}{1+r^2}\frac{2k^{\rm h}k^{\rm c}\phi\Delta\phi + O'(\Delta\phi^2)}{\mathcal{L}^{\rm eq}} \\ \approx \frac{2k^{\rm h}k^{\rm c}\phi\Delta\phi}{(1-N^2)\left(k^{\rm h}+k^{\rm c}\right)^2\left(1-\phi^2\right)}, \tag{S50}$$

where O and O' are higher order terms and the expansion of $\mathcal{L}^{\rm eq}$ yields

$$\mathcal{L}^{\rm eq} \approx \left(1-N^2\right)\left[\left(k^{\rm h}+k^{\rm c}\right)^2\left(1-\phi^2\right)+2k^{\rm c}\left(k^{\rm h}+k^{\rm c}\right)\phi\Delta\phi\right].$$

We find that both linear coefficients are negative and $\mathcal{S}_1^0 = r^2\mathcal{S}_2^0$. For $r > 1$, the negative contribution from dot 1 (weaker coupling) is stronger. As the second-order coefficients are positive for $\phi\Delta\phi > 0$ and stronger than the linear coefficients for very small $\Delta\phi$, the nonlinear contribution may overcome the linear response to make the quantum conductance positive.

Approaching to $\phi^{\rm h} = \phi^{\rm c} = \pm 1$, the leading order of $\mathcal{L}^{\rm eq}$ becomes linear in $\Delta\phi$, thus $\mathcal{S}_d^1$ remains finite, while $\mathcal{S}_d^0$ goes to zero. Therefore, a strong enhancement of the current is expected.

S4. FULLY SYMMETRIC CASE

We consider the most symmetric case with $\phi^{\rm h} = \phi^{\rm c} = \phi$ in the r-symmetric configuration, where we find simple relations as $W_2 = r^2 W_1$, $\overline{W}_2 = r^2 \overline{W}_1$, $\Phi = r\phi W_1$, and $\overline{\Phi} = r\phi \overline{W}_1$. Then, the Liouville matrix becomes

$$\mathsf{L} = \begin{pmatrix} -(1+r^2)W_1 & \overline{W}_1 & r^2\overline{W}_1 & r\phi\overline{W}_1 & r\phi\overline{W}_1 \\ W_1 & -\overline{W}_1 & 0 & \frac{-r\phi\overline{W}_1}{2} & \frac{-r\phi\overline{W}_1}{2} \\ r^2 W_1 & 0 & -r^2\overline{W}_1 & \frac{-r\phi\overline{W}_1}{2} & \frac{-r\phi\overline{W}_1}{2} \\ r\phi W_1 & \frac{-r\phi\overline{W}_1}{2} & \frac{-r\phi\overline{W}_1}{2} & \frac{-(1+r^2)\overline{W}_1}{2} & 0 \\ r\phi W_1 & \frac{-r\phi\overline{W}_1}{2} & \frac{-r\phi\overline{W}_1}{2} & 0 & \frac{-(1+r^2)\overline{W}_1}{2} \end{pmatrix}. \tag{S51}$$

The eigenvectors and the corresponding eigenvalues of L can be obtained from more general results in Sec. S2 or by directly diagonalizing Eq. (S51). The first three eigenvectors are given as

$$\mathbf{v}_1^{\rm T} = (\overline{\alpha}, \alpha, \alpha, 0, 0)\ , \mathbf{v}_2^{\rm T} = (0, 0, 0, 1, -1)\ , \mathbf{v}_3^{\rm T} = \left(0, 1, -1, \frac{r^2-1}{2r\phi}, \frac{r^2-1}{2r\phi}\right), \tag{S52}$$

where $\alpha = W_1/(2W_1 + \overline{W}_1)$, $\bar{\alpha} = 1 - 2\alpha$, and the corresponding eigenvalues are $\lambda_1 = 0, \lambda_2 = -\frac{1+r^2}{2}\overline{W}_1$ and $\lambda_3 = -\frac{1+r^2}{2}\overline{W}_1$, respectively. The fourth and the fifth eigenvectors are given as

$$\mathbf{v}_{4(5)}^{\rm T} = \left(1, -\frac{\lambda_{4(5)} + r^2(W_1 + \overline{W}_1) - W_1}{2\lambda_{4(5)} + (1+r^2)\overline{W}_1}, -\frac{\lambda_{4(5)} + W_1 + \overline{W}_1 - r^2 W_1}{2\lambda_{4(5)} + (1+r^2)\overline{W}_1}, \frac{r\phi\left(2W_1 + \overline{W}_1\right)}{2\lambda_{4(5)} + (1+r^2)\overline{W}_1}, \frac{r\phi\left(2W_1 + \overline{W}_1\right)}{2\lambda_{4(5)} + (1+r^2)\overline{W}_1}\right) \tag{S53}$$

and the corresponding eigenvalues are

$$\lambda_4 = \frac{-\left(1+r^2\right)\left(W_1 + \overline{W}_1\right) + U}{2}, \quad \lambda_5 = \frac{-\left(1+r^2\right)\left(W_1 + \overline{W}_1\right) - U}{2} \tag{S54}$$

with $U = \sqrt{\left[(1+r^2)\left(W_1 + \overline{W}_1\right)\right]^2 - 4r^2(1-\phi^2)\left(2W_1\overline{W}_1 + \overline{W}_1^2\right)}$.

One can notice that the maximum interference condition ($|\phi| = 1$) yields $\lambda_4 = 0$, implying that the steady state is not determined uniquely. In fact, any state spanned by $\mathbf{v}_1$ and $\mathbf{v}_4$ can become a steady state, depending on the initial condition. For $|\phi| < 1$, all four eigenvalues are negative except $\lambda_1 = 0$, so we have a unique steady state represented $\mathbf{v}_1$, which is identical to the classical steady state at $\phi = 0$.

Defining a matrix $\mathsf{V} = (\mathbf{v}_1, \mathbf{v}_2, \mathbf{v}_3, \mathbf{v}_4, \mathbf{v}_5)$ with its inverse V^{-1}, the formal solution $\mathbf{P}(t)$ at time t with an initial vector $\mathbf{P}(0) = (\rho_{00}(0), \rho_{11}(0), \rho_{22}(0), \rho_{12}(0), \rho_{21}(0))^{\rm T}$, reads

$$\mathbf{P}(t) = \mathsf{V}\mathsf{V}^{-1} e^{\mathsf{L}t}\, \mathsf{V}\mathsf{V}^{-1}\mathbf{P}(0)\,, \tag{S55}$$

or $\mathbf{P}(t) = \mathsf{V}\left(1, \chi_2 e^{\lambda_2 t}, \chi_3 e^{\lambda_3 t}, \chi_4 e^{\lambda_4 t}, \chi_5 e^{\lambda_5 t}\right)^{\mathrm{T}}$, where we used $\rho_{00}(0) + \rho_{11}(0) + \rho_{22}(0) = 1$. All χ_i's can be calculated from Eq. (S55) if the initial condition $\mathbf{P}(0)$ is given.

Let us consider the simple case of $r = 1$, where the eigenvectors and the eigenvalues are given by $\mathbf{v}_1^{\mathrm{T}} = (\bar{\alpha}, \alpha, \alpha, 0, 0)$, $\mathbf{v}_2^{\mathrm{T}} = (0, 0, 0, 1, -1)$, $\mathbf{v}_3^{\mathrm{T}} = (0, 1, -1, 0, 0)$, $\mathbf{v}_4^{\mathrm{T}} = \left(1, -\frac{1}{2}, -\frac{1}{2}, \frac{U_1+W_1}{2\phi\overline{W}_1}, \frac{U_1+W_1}{2\phi\overline{W}_1}\right)$, and $\mathbf{v}_5^{\mathrm{T}} = \left(1, -\frac{1}{2}, -\frac{1}{2}, \frac{W_1-U_1}{2\phi\overline{W}_1}, \frac{W_1-U_1}{2\phi\overline{W}_1}\right)$, with $\lambda_1 = 0$, $\lambda_2 = -\overline{W}_1$, $\lambda_3 = -\overline{W}_1$, $\lambda_4 = -(W_1 + \overline{W}_1) + U_1$ and $\lambda_5 = -(W_1 + \overline{W}_1) - U_1$, where $U_1 = \sqrt{(W_1 + \overline{W}_1)^2 - (1 - \phi^2)2W_1\overline{W}_1 + \overline{W}_1^2)}$. Then the inverse matrix V^{-1} is obtained as

$$\mathsf{V}^{-1} = \begin{pmatrix} 1 & 1 & 1 & 0 & 0 \\ 0 & 0 & 0 & \frac{1}{2} & -\frac{1}{2} \\ 0 & \frac{1}{2} & -\frac{1}{2} & 0 & 0 \\ \frac{\alpha(U_1-W_1)}{U_1} & -\frac{\bar{\alpha}(U_1-W_1)}{2U_1} & -\frac{\bar{\alpha}(U_1-W_1)}{2U_1} & \frac{\phi\overline{W}_1}{2U_1} & \frac{\phi\overline{W}_1}{2U_1} \\ \frac{\alpha(U_1+W_1)}{U_1} & -\frac{\bar{\alpha}(U_1+W_1)}{2U_1} & -\frac{\bar{\alpha}(U_1+W_1)}{2U_1} & -\frac{\phi\overline{W}_1}{2U_1} & -\frac{\phi\overline{W}_1}{2U_1} \end{pmatrix}. \tag{S56}$$

If the initial condition is given by $\rho_{11}(0) = \rho_{22}(0)$ and $\rho_{12}(0) = \rho_{21}(0)$, Eq. (S55) is simplified since $\chi_2 = \chi_3 = 0$ and thus $\rho_{11}(t) = \rho_{22}(t)$ and $\rho_{12}(t) = \rho_{21}(t)$. It is straightforward to obtain the dynamic equation

$$\begin{pmatrix} \rho_{11}(t) \\ \rho_{12}(t) \end{pmatrix} = \alpha\mathbf{A}(\phi, t) + \mathsf{M}(\phi, t)\begin{pmatrix} \rho_{11}(0) \\ \rho_{12}(0) \end{pmatrix}, \tag{S57}$$

where the vector $\mathbf{A}$ is given by

$$\mathbf{A}(\phi, t) = \frac{1}{2}\begin{pmatrix} 2 - R_+(\phi, t) + \frac{W_1}{U_1}R_-(\phi, t) \\ \frac{\phi(2W_1+\overline{W}_1)}{U_1}R_-(\phi, t) \end{pmatrix}, \tag{S58}$$

and the Matrix M,

$$\mathsf{M}(\phi, t) = \frac{1}{2}\begin{pmatrix} R_+(\phi, t) - \frac{W_1}{U_1}R_-(\phi, t) & -\frac{\phi\overline{W}_1}{U_1}R_-(\phi, t) \\ -\frac{\phi(2W_1+\overline{W}_1)}{U}R_-(\phi, t) & R_+(\phi, t) + \frac{W_1}{U_1}R_-(\phi, t) \end{pmatrix}. \tag{S59}$$

Here, $R_\pm(\phi, t) = e^{\lambda_4 t} \pm e^{\lambda_5 t}$. The data in Fig. 3 of the main text are calculated from Eq. (S57) with the initial state of $\rho_{11}(0) = \rho_{12}(0) = 0$.

At the singular point ($\phi = 1$), the multiple steady states emerge, depending on the initial condition. As the two eigenvalues ($\lambda_1 = \lambda_4$) become zero, there should be a conservation law associated with λ_4, in addition to the probability conservation responsible for λ_1. From the structure of the Liouville matrix in Eq. (S51), one can easily find the conservation law of $r^2\dot{\rho}_{11} + \dot{\rho}_{22} - r\dot{\rho}_{12} - r\dot{\rho}_{21} = 0$ for $\phi = 1$. This implies that the quantity $r^2\rho_{11}(t) + \rho_{22}(t) - r\rho_{12}(t) - r\rho_{21}(t) = I_0$ does not change

in time. Using the relation of Eq. (5) of the main text and this conservation law, we obtain the multiple fixed points as

$$\rho_{11}(\infty) = \alpha - [r\bar{\alpha} - \frac{1-r^2}{r}\alpha]\rho_{12}(\infty)\,, \quad \rho_{22}(\infty) = \alpha - [\frac{\bar{\alpha}}{r} + \frac{1-r^2}{r}\alpha]\rho_{12}(\infty)\,,$$
$$\rho_{12}(\infty) = \rho_{21}(\infty) = \frac{r}{1+r^2}\frac{1}{1-\alpha}\left(\alpha - \frac{I_0}{1+r^2}\right)\,, \tag{S60}$$

where $I_0 = r^2\rho_{11}(0) + \rho_{22}(0) - r\rho_{12}(0) - r\rho_{21}(0)$. Similarly, we get the extra conservation of $r^2\rho_{11}(t) + \rho_{22}(t) + r\rho_{12}(t) + r\rho_{21}(t) = I_0'$ for $\phi = -1$ and the corresponding multiple fixed points are given as

$$\rho_{11}(\infty) = \alpha + [r\bar{\alpha} - \frac{1-r^2}{r}\alpha]\rho_{12}(\infty)\,, \quad \rho_{22}(\infty) = \alpha + [\frac{\bar{\alpha}}{r} + \frac{1-r^2}{r}\alpha]\rho_{12}(\infty)\,,$$
$$\rho_{12}(\infty) = \rho_{21}(\infty) = -\frac{r}{1+r^2}\frac{1}{1-\alpha}\left(\alpha - \frac{I_0'}{1+r^2}\right)\,, \tag{S61}$$

where $I_0' = r^2\rho_{11}(0) + \rho_{22}(0) + r\rho_{12}(0) + r\rho_{21}(0)$.

We can also calculate the steady-state currents. From Eqs. (S37)-(S40), we obtain

$$\Psi_1 = \frac{\overline{\Phi}}{|\mathsf{L}_0|}(1+r^2)\left(w^{\rm h}_{1+}\overline{W}_1 - w^{\rm h}_{1-}W_1\right) = \phi\frac{1+r^2}{r}J^{\rm cl}_1\,,$$
$$\Psi_2 = \frac{\overline{\Phi}}{|\mathsf{L}_0|}\left(1+\frac{1}{r^2}\right)\left(w^{\rm h}_{2+}\overline{W}_2 - w^{\rm h}_{2-}W_2\right) = \phi\frac{1+r^2}{r}J^{\rm cl}_2\,, \tag{S62}$$

where

$$J^{\rm cl}_1 = \frac{2\pi|g^{\rm h}_1|^2|g^{\rm c}_1|^2\Delta N}{|g^{\rm h}_1|^2\widetilde{N}^{\rm h} + |g^{\rm c}_1|^2\widetilde{N}^{\rm c}}\,, \qquad J^{\rm cl}_2 = r^2 J^{\rm cl}_1\,, \tag{S63}$$

with $\widetilde{N}^a = 1 + N^a$. For $|\phi| < 1$, the classical solution becomes the unique steady state ($\rho_{12}(\infty) = 0$), thus the steady-state current is purely classical. However, at $|\phi| = 1$, we have a nonzero $\rho_{12}(\infty)$ in Eqs. (S60) and (S61) and the steady-state current contains the quantum part as $J_d(\infty) = J^{\rm cl}_d + \Psi_d\rho(\infty)$, thus, for $\phi = \pm 1$,

$$J_d(\infty) = J^{\rm cl}_d\left(1 \pm \frac{1+r^2}{r}\rho_{12}(\infty)\right)\,. \tag{S64}$$

Note that these currents are the same for $\phi = \pm 1$ with the initial conditions of $I_0 = I_0'$. In equilibrium, the quantum current vanishes as well as the classical current even if $\rho_{12}(\infty) \neq 0$, because the quantum speed Ψ_d vanishes at $\Delta N = 0$ as in Eq. (S62).

---

[1] H.-P. Breuer, and F. Petruccione, *The theory of open quantum systems* (Oxford University Press, New York, 2002).

[2] U. Harbola, M. Esposito, and S. Mukamel, Phys. Rev. B **74**, 235309 (2006).

[3] G. Schaller, G. Kießlich, and T. Brandes Phys. Rev. B **80**, 245107 (2009).

[4] G. B. Cuetara, M. Esposito, and G. Schaller, Entropy **18**, 447 (2016).

[5] M. Q. Weng, EPL 85, 17003 (2009).

[6] T. Hayashi, T. Fujisawa, H. D. Cheong, Y. H. Jeong, and Y. Hirayama, Phys. Rev. Lett. **91**, 226804 (2003).

[7] W. G. van der Wiel, S. De Franceschi, J. M. Elzerman, T. Fujisawa, S. Tarucha, and L. P. Kouwenhoven, Rev. Mod. Phys. **75**, 1 (2003).

[8] A. W. Holleitner, C. R. Decker, H. Qin, K. Eberl, and R. H. Blick, Phys. Rev. Lett. **87**, 256802 (2001).

[9] A. W. Holleitner, R. H. Blick, A. K. Hüttel, K. Eberl, and J. P. Kotthaus, Science **297**, 70 (2002).

[10] J. C. Chen, A. M. Chang, and M. R. Melloch, Phys. Rev. Lett. **92**, 176801 (2004).